sulfated cholecystokinin octapeptide (CCK-8S) both in vivo and in vitro.

RESEARCH DESIGN AND METHODS

ICAM-1$^{-/-}$ mice studies. Male ICAM-1$^{-/-}$ mice (C57BL/6J background) (15) were purchased from The Jackson Laboratory (Bar Harbor, ME). Male C57BL/6J (ICAM-1$^{+/+}$) mice were used as controls. WT and ICAM-1$^{-/-}$ mice aged 8 weeks were divided into the following four groups (n = 5 each): *1*) nondiabetic WT mice, *2*) nondiabetic ICAM-1$^{-/-}$ mice, *3*) streptozotocin (STZ)-induced diabetic WT mice, and *4*) STZ-induced diabetic ICAM-1$^{-/-}$ mice. STZ was purchased from Sigma-Aldrich (St. Louis, MO). Mice in the diabetic groups received two intraperitoneal doses of STZ (each 100 mg/kg) given 7 days apart. Blood glucose levels were determined 7 days after STZ injection, and only mice with

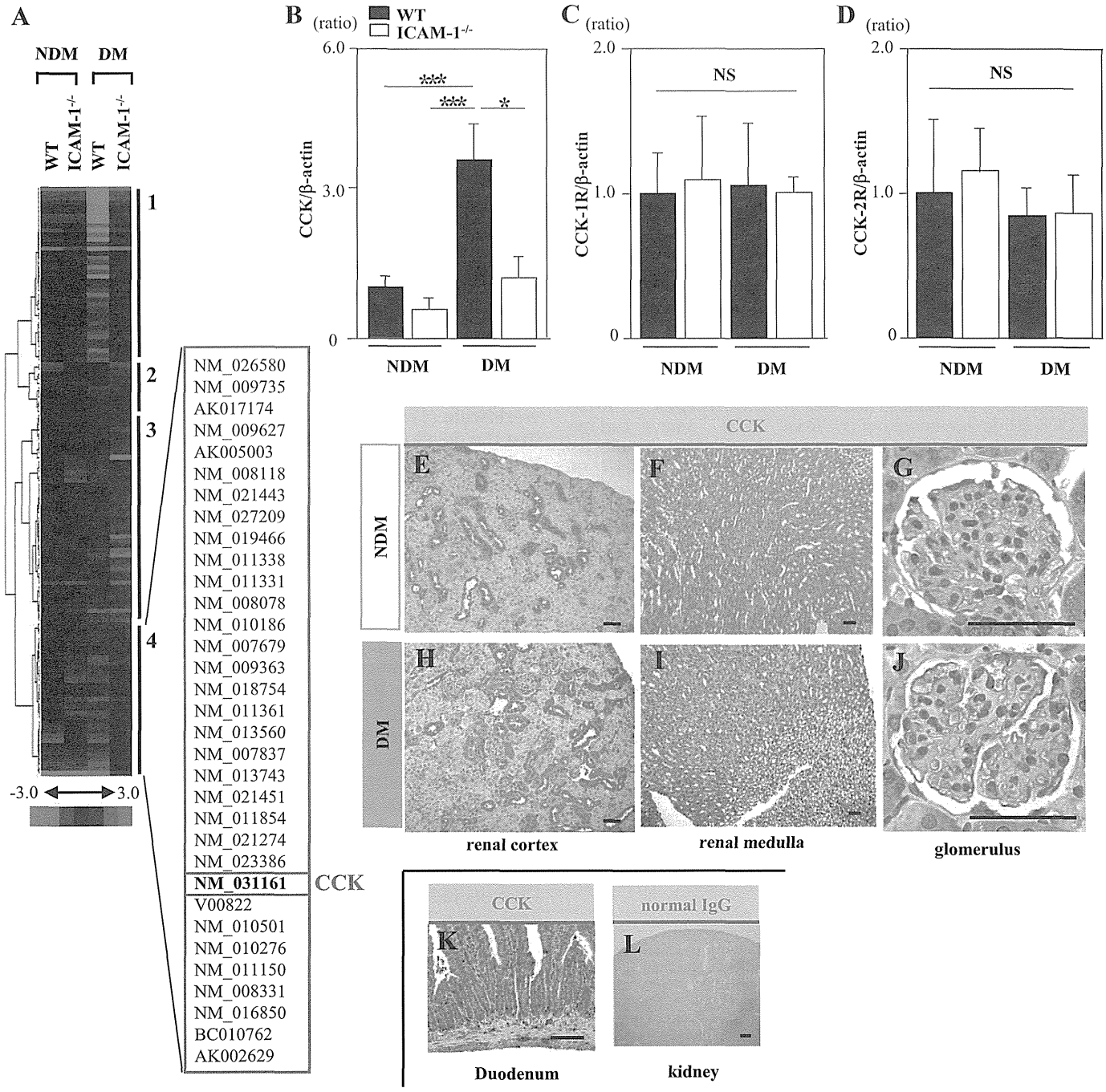

FIG. 1. The expression and distribution of CCK in kidney tissues of mice. *A*: Cluster analysis of differentially expressed genes comparing NDM WT and ICAM-1$^{-/-}$ mice and STZ-induced DM WT and ICAM-1$^{-/-}$ mice (n = 5/group). The dendrogram on the left of the cluster shows the relatedness of the change in gene expression. On the right of the cluster diagram, four groups of genes (1–4) are identified based on their gene expression changes. The list of constitutive genes involved in cluster 4 is given using the GenBank accession numbers. CCK was included in this cluster. *B*: CCK mRNA expression in the renal cortices was significantly increased in diabetic WT mice and significantly reduced to a nondiabetic level in diabetic ICAM-1$^{-/-}$ mice. *C* and *D*: The mRNA expressions of CCK-1R and CCK-2R were almost the same among the four groups. Values (means ± SEM) are presented as the ratio of nondiabetic WT. Data shown are representative of three separate experiments performed with five mice per group. *E–G*: Immunohistological staining of renal tissue specimens obtained from nondiabetic WT mice. The CCK-positive area was mainly observed in the distal tubules (*E*) and collecting ducts (*F*) and weakly in glomeruli (*G*). *H–J*: Immunohistological staining of kidney tissue specimens obtained from diabetic WT mice. The distal tubules (*H*) and glomeruli (*J*) were stained more intensely compared with those in the nondiabetic WT mice. A duodenal tissue specimen was used as a positive control (*K*). Normal IgG was also used as a negative control (*L*). Scale bars, 50 μm. *P < 0.05. ***P < 0.001. NS, P > 0.05. (A high-quality digital representation of this figure is available in the online issue.)

blood glucose concentrations >16 mmol/L were used in the study. Nondiabetic WT and ICAM-1$^{-/-}$ mice received citrate buffer injections only. All animal procedures were performed according to the guidelines as described previously (16). Three months after the induction of diabetes, all mice were killed, and the kidneys were harvested.

Oligonucleotide microarray. Total RNA was extracted from each specimen of the renal cortex using the standard protocol included with the RNeasy Midi Kit (Qiagen, Valencia, CA) at 3 months. Preparation of biotin-labeled target cRNA and hybridization of probe arrays (CodeLink UniSet Mouse I Bioarray) were performed according to the manufacturer's instructions (Amersham Biosciences, Uppsala, Sweden) (Gene Expression Omnibus accession numbers are available in the Supplementary Data).

Microarray data analysis. The criteria for selecting genes that were induced or reduced by a diabetic state were as follows: *1*) the gene flags were "true," and *2*) the ratio of the gene expression level in diabetic WT mice to that in diabetic ICAM-1$^{-/-}$ mice was >2 or <0.5. We then selected 193 genes for further analysis. All normalized data values were replaced to log base 2 and subjected to hierarchical clustering as described previously (16).

CCK receptor knockout mice studies. CCK-1R$^{-/-}$, CCK-2R$^{-/-}$, and CCK-1R$^{-/-}$,-2R$^{-/-}$ mice (C57BL/6J background) (17) were obtained from the Tokyo Metropolitan Institute of Gerontology. CCK-1R$^{-/-}$ mice and CCK-2R$^{-/-}$ mice were generated as described previously (18,19). C57BL/6J (CCK-1R$^{+/+}$,-2R$^{+/+}$) mice were used as controls. Male WT and CCK-1R$^{-/-}$,-2R$^{-/-}$ mice aged 8 weeks were divided into four groups (n = 7 each): *1*) nondiabetic WT mice, *2*) nondiabetic CCK-1R$^{-/-}$,-2R$^{-/-}$ mice, *3*) STZ-induced diabetic WT mice, and *4*) diabetic CCK-1R$^{-/-}$,-2R$^{-/-}$ mice. Diabetes was induced as described above. Blood pressure, blood glucose, A1C, serum creatinine, urine creatinine, and urinary albumin were measured as described previously (16). Three months after the induction of diabetes, all mice were killed, and the kidneys were harvested as described previously (16). Male CCK-1R$^{-/-}$ and CCK-2R$^{-/-}$ mice aged 8 weeks (n = 7 each) were also used for comparison of albuminuria after induction of diabetes.

Bone marrow transplantation studies. Bone marrow transplantation (BMT) was performed as described previously (20,21). Briefly, male WT and CCK-1R$^{-/-}$ mice aged 7–9 weeks received 9 Gy of total body irradiation. Postirradiated male CCK-1R$^{-/-}$ mice received a bone marrow transplant from WT mice (WT→1R$^{-/-}$; n = 6). Postirradiated WT mice received a BMT from CCK-1R$^{-/-}$ mice (1R$^{-/-}$→WT; n = 6) or WT mice (WT→WT; n = 4). Four weeks after BMT, diabetes was induced in all mice by STZ as described above. Four weeks after the induction of diabetes, all mice were killed. DNA was isolated from bone marrow extracts of all recipient mice using a DNeasy Blood & Tissue Kit (Qiagen). The chimerism was confirmed by PCR (Supplementary Fig. 1) at the termination of the study as described previously (22). The specific oligonucleotide primer sequences are shown in Supplementary Table 1.

Interventional animal studies. Male Sprague-Dawley (SD) rats were purchased from CLEA Japan (Tokyo, Japan). SD rats aged 4 weeks were divided into three groups (n = 7 each): *1*) nondiabetic control group (NDM), *2*) STZ-induced diabetic group (DM), and *3*) CCK-8S–treated diabetic group (DM-CCK). At the age of 5 weeks, rats chosen for the DM and DM-CCK groups were injected intravenously with STZ (65 mg/kg body wt) in citrate buffer (pH 4.5). Rats in the NDM group received citrate buffer injections only. At the age of 6 weeks, Alzet osmotic minipumps (Durect Corporation, Cupertino, CA) were implanted subcutaneously in the backs of all the rats. Rats in the DM-CCK group were continuously infused with CCK-8S (Bachem, Bubendorf, Switzerland) dissolved in 0.9% saline and given at a rate of 5 μg CCK-8S/kg · h^{-1}. Animals in the NDM and DM groups were continuously infused with 0.9% saline only. Food intake was calculated as the average over 3 days. Serum CCK concentration in both diabetic groups was measured using the CCK Enzyme Immunoassay Kit (RayBiotech, Norcross, GA) according to the manufacturer's instructions. Because the life expectancy of the osmotic pumps was 4 weeks, all pumps were replaced with new filled pumps when the rats reached the age of 10 weeks. Eight weeks after the induction of diabetes, all rats were killed, and the kidneys were harvested as described previously (16). Glomeruli were isolated from the left kidney by a previously developed sieving technique (23).

Histological analysis. Periodic acid-methenamine silver (PAM)-stained sections were analyzed as described previously (24). To evaluate the glomerular size and mesangial matrix area, we examined 10 randomly selected glomeruli per mouse and 15 randomly selected glomeruli per rat under high magnification (×400). Quantitative analysis for all staining was performed in a blinded manner.

Immunoperoxidase staining. Immunoperoxidase staining was performed as described previously (4). Primary antibodies were monoclonal antibody against rat monocytes/macrophages (ED1, 1:50; Serotec, Oxford, U.K.), polyclonal antibody against WT-1 (1:50; Santa Cruz Biotechnology, Santa Cruz, CA), or polyclonal antibody against cholecystokinin octapeptide (1:500; Phoenix Pharmaceuticals, Belmont, CA), all of which were applied for 12 h at 4°C. Secondary antibodies were biotin-labeled goat anti-mouse IgG (Jackson ImmunoResearch Laboratories, West Grove, PA) or biotin-labeled goat anti-rabbit IgG (Vector Laboratories, Burlingame, CA) for 60 min at room temperature. Intraglomerular ED1-positive cells or WT-1–positive cells were counted in 20 glomeruli per animal (n = 4/group).

Immunohistochemical staining. Immunofluorescence staining was performed using the methods described previously (5). Rabbit antitype IV collagen Ab (1:200; LSL, Tokyo, Japan) was used for the primary reactions for 60 min at room temperature, followed by a second reaction with fluorescein isothicyanate-conjugated goat anti-rabbit IgG (H+L; Zymed Laboratories, San Francisco, CA) for 30 min at room temperature. The immunofluorescence intensity of type IV collagen was quantified as described previously (24). We evaluated 15 glomeruli per animal (n = 4/group).

RNA extraction and quantitative real-time PCR. RNA extraction, real-time PCR, and visualization of gene expression were performed as described previously (24). The specific oligonucleotide primer sequences are shown in Supplementary Table 2.

Nuclear protein extract. Nuclear proteins were extracted from kidney tissues with a nuclear extract kit (Active Motif, Carlsbad, CA) according to the manufacturer's instructions.

Nuclear factor-κB activity measurement. Nuclear factor-κB (NF-κB) p65-dependent DNA-binding activity was determined by TransAM NFκB p65 (Active Motif) according to the manufacturer's instructions.

Cell culture. THP-1 cells were obtained from DS Pharma Biomedical (Osaka, Japan) and cultured according to the manufacturer's instructions. PBS without calcium and magnesium [PBS (−)] was purchased from Invitrogen (Carlsbad, CA).

Tumor necrosis factor-α mRNA expression in THP-1 cells. THP-1 cells were precultured in the RPMI 1640 (without glucose) medium supplemented with 10% FCS and 5.5 mmol/L D-glucose (Sigma-Aldrich) for 72 h. The cells were centrifuged, washed in PBS (−), centrifuged, and serum starved for 12 h in RPMI 1640 medium containing 5.5 mmol/L D-glucose. After starvation, the cells were adjusted to a cell density of 4 × 10^5 cells/mL in RPMI 1640 medium containing 5.5 mmol/L D-glucose and 1% FCS and placed in six-well plates (Falcon, Franklin Lakes, NJ). A control scrambled peptide (H-Gly-Asp-Tyr-Asp-Met-Trp-Met-Phe-NH$_2$) and proglumide (a nonselective CCK receptor antagonist that interacts with both CCK receptors and can cross brain–blood barrier) were purchased from Sigma-Aldrich. The cells were exposed to the following stimuli (n = 5/group): *1*) 5.5 mmol/L D-glucose (normal glucose [NG]); *2*) 15 mmol/L

TABLE 1
Metabolic characteristics of WT mice and CCK receptor knockout mice (3 months after induction of diabetes)

	Nondiabetic groups		Diabetic groups			
	WT	1R$^{-/-}$,-2R$^{-/-}$	WT	1R$^{-/-}$,-2R$^{-/-}$	1R$^{-/-}$	2R$^{-/-}$
n	7	7	7	7	7	7
SBP, mmHg	105.4 ± 1.1	109.7 ± 1.7	106.5 ± 1.3	105.1 ± 2.1	101.2 ± 2.1	99.9 ± 1.8
BW, g	31.6 ± 0.8	31.2 ± 0.4	26.7 ± 0.3†&	25.4 ± 0.8*§	24.0 ± 0.6*§	25.8 ± 0.6*§
Kidney weight, mg/g BW	10.2 ± 0.2	12.4 ± 0.4†	12.5 ± 0.3†	14.8 ± 0.35*‡&	15.2 ± 0.4*‡&	16.2 ± 1.0*‡&
A1C, %	3.8 ± 0.1	3.2 ± 0.1	9.8 ± 0.3*§	9.9 ± 0.4*§	9.1 ± 0.2*§	9.5 ± 0.4*§
Cr, mg/dL	0.12 ± 0.01	0.12 ± 0.01	0.11 ± 0.01	0.11 ± 0.01	0.10 ± 0.01	0.09 ± 0.01
Ccr, mL · min^{-1} · g BW^{-1}	7.0 ± 0.7	3.7 ± 0.3	17.7 ± 2.7†&	17.1 ± 2.8†&	18.1 ± 2.8†&	14.6 ± 3.7

Data are means ± SEM. BW, body weight; Ccr, creatinine clearance; Cr, creatinine; SBP, systolic blood pressure. †P < 0.05 vs. nondiabetic WT group. &P < 0.05 vs. nondiabetic CCK-1R$^{-/-}$,-2R$^{-/-}$ group. *P < 0.001 vs. nondiabetic WT group. §P < 0.001 vs. nondiabetic CCK-1R$^{-/-}$,-2R$^{-/-}$ group. ‡P < 0.05 vs. diabetic WT group.

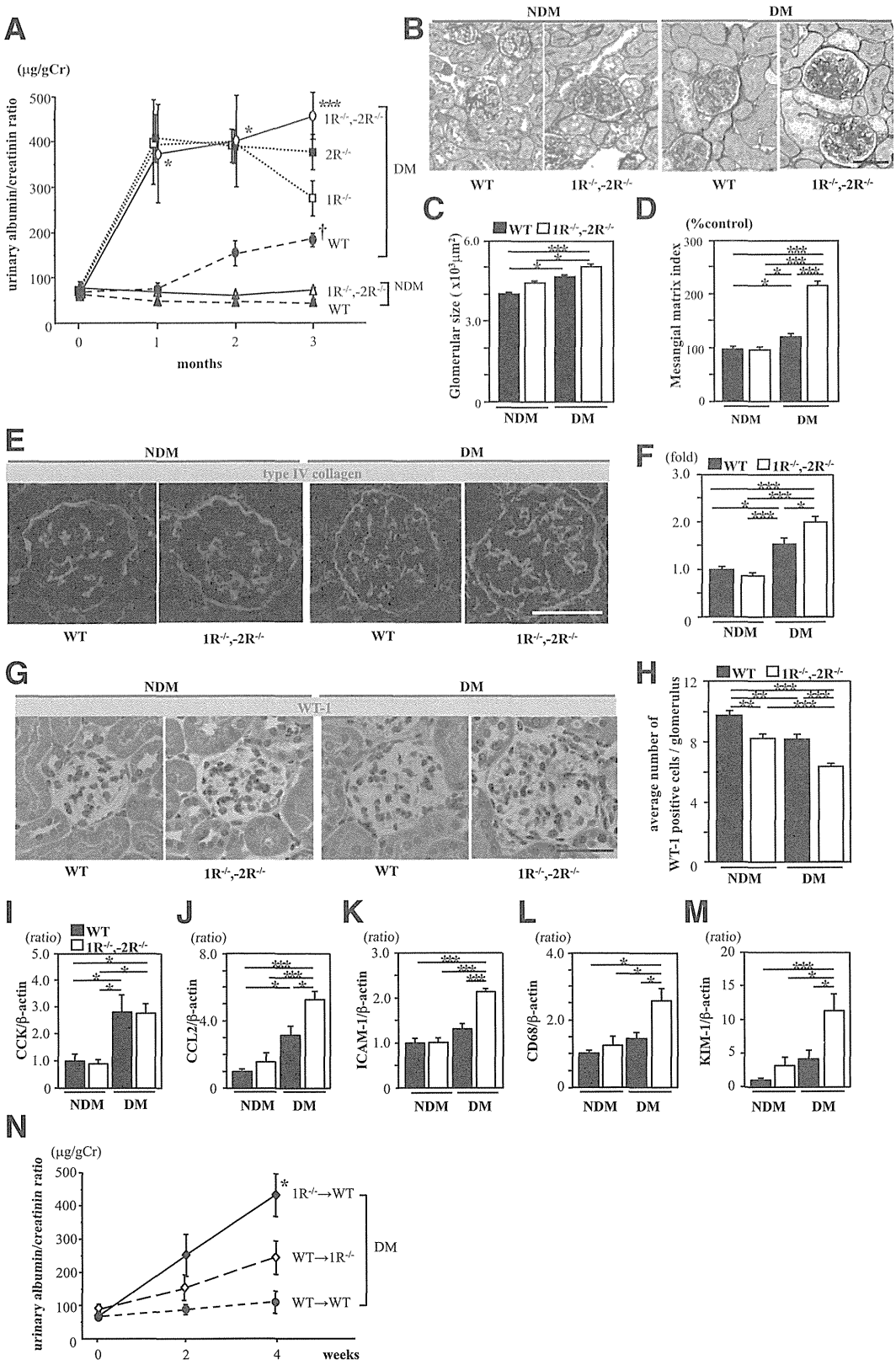

FIG. 2. Diabetic CCK-1R$^{-/-}$,-2R$^{-/-}$ mice exhibited increased albuminuria and enhanced proinflammatory genes in the kidney. *A*: Time course of urinary albumin/creatinine ratio (UACR). The UACR of diabetic CCK-1R$^{-/-}$,-2R$^{-/-}$ mice (○) was markedly increased as compared with that of diabetic WT mice (●) (n = 7/group). The UACR of CCK-1R$^{-/-}$,-2R$^{-/-}$ mice was higher than that of CCK-1R$^{-/-}$ mice (□) or CCK-2R$^{-/-}$ mice (■) at 3 months. *P < 0.05 vs. diabetic WT and nondiabetic groups; ***P < 0.001 vs. diabetic WT and nondiabetic groups; †P < 0.05 vs. nondiabetic groups. *B*: PAM staining of the kidney at 3 months. Scale bars, 50 μm. *C*: Glomerular hypertrophy was observed in both diabetic groups as compared with nondiabetic WT mice (n = 5/group). *P < 0.05; ***P < 0.001. *D*: The mesangial matrix index, calculated by the PAM-positive area in the tuft area, was significantly increased in diabetic CCK-1R$^{-/-}$,-2R$^{-/-}$ mice as compared with the other three groups. Ten randomly selected glomeruli per mouse were examined (n = 5/group). *P < 0.05; ***P < 0.001. *E*: Expression of type IV collagen in kidney tissue. Scale bars, 50 μm. *F*: Collagen IV-positive area in glomeruli (folds versus the nondiabetic WT group). Type IV collagen was significantly increased in the diabetic CCK-1R$^{-/-}$,-2R$^{-/-}$

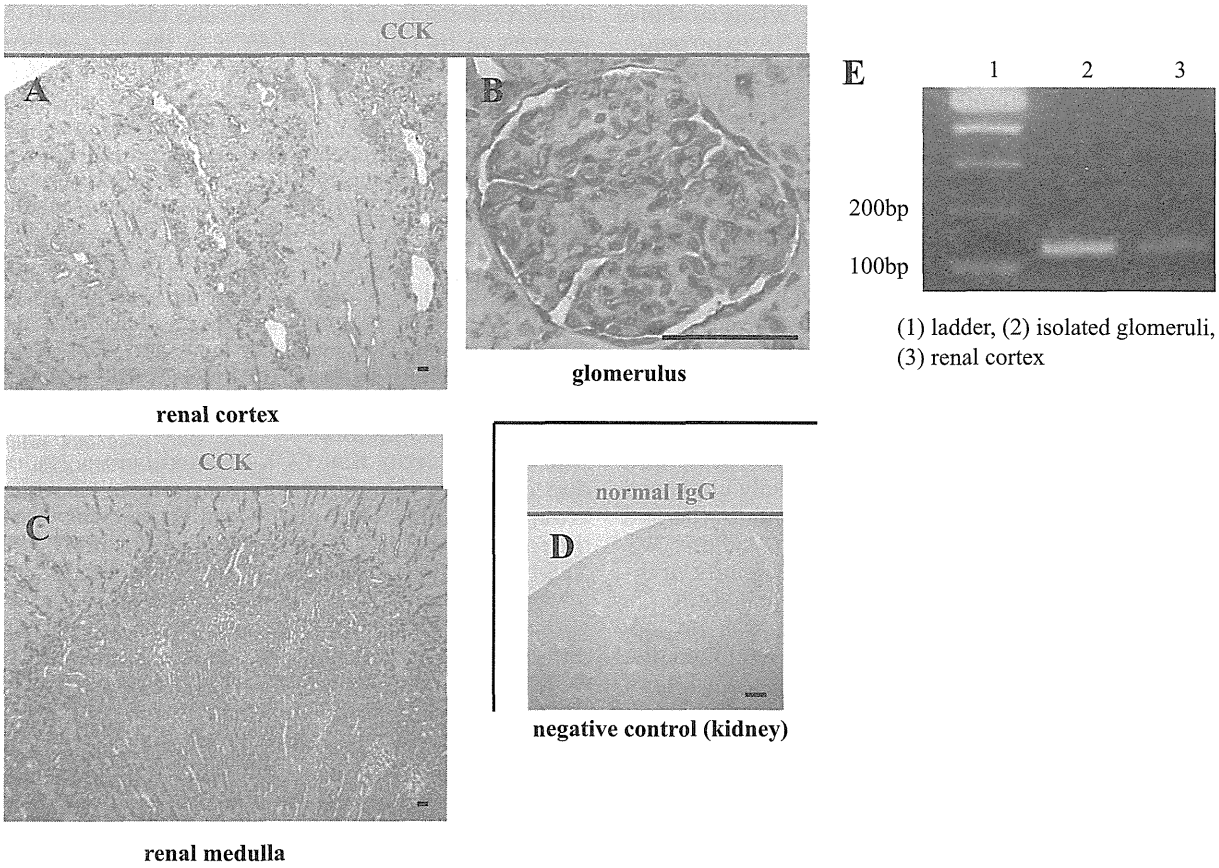

FIG. 3. Distribution of CCK in the rat renal tissues. *A–D*: Immunohistological staining of renal tissue specimens obtained from nondiabetic rats. The CCK-positive area was mainly observed in the distal tubules (*A*), glomeruli (*B*), and collecting ducts (*C*). Scale bars, 50 μm. Normal IgG was also used as a negative control (*D*). Scale bar, 500 μm. *E*: CCK mRNA expression was observed in isolated glomeruli and the renal cortex obtained from nondiabetic rats. (A high-quality digital representation of this figure is available in the online issue.)

D-glucose (high glucose [HG]); *3*) 5.5 mmol/L D-glucose with 9.5 mmol/L mannitol (osmotic control [Mn]); *4*) HG with scrambled peptide (10^{-6} M); *5*) HG with CCK-8S (10^{-8} M); *6*) HG with CCK-8S (10^{-7} M); *7*) HG with CCK-8S (10^{-6} M); and *8*) HG with CCK-8S (10^{-6} M) and proglumide (10^{-5} M).

CCK-8S and proglumide were added daily. After incubation for 72 h, total RNA was extracted, and quantitative real-time RT-PCR was performed as described above. Tumor necrosis factor-α (TNF-α) mRNA expression levels were normalized by β-actin in each sample. Values (means ± SEM) were expressed as the ratios of average values in HG.

Cell migration assays. THP-1 cell migration was analyzed with a modified Boyden chamber assay using a 24-well transwell with 5.0-μm pores (Corning Life Sciences, Corning, NY) as described previously (25,26). THP-1 cells were preincubated for 24 h in serum-free RPMI 1640 supplemented with 0.1% bovine serum albumin (Sigma-Aldrich). After starvation, CCK-8S, scrambled peptide, or proglumide was added to THP-1 cells at different concentrations, and the cells were added to the top chamber. CCK-8S or scrambled peptide was incubated from 15 min before addition to the top chamber, and proglumide was added 15 min before addition of CCK-8S. The medium in the lower well contained 100 ng/mL of recombinant human CC chemokine ligand 2 (CCL2; R&D Systems, Minneapolis, MN). Cells that migrated to the bottom side of the membrane were quantitated by CyQuant DNA-binding fluorescence (Invitrogen) according to the manufacturer's instructions (n = 6 each).

Statistical analysis. All values are expressed as the means ± SEM. Differences between groups were examined for statistical significance using one-way ANOVA followed by Scheffe's test. A P value <0.05 was considered statistically significant.

RESULTS

Enhanced CCK expression in the kidney tissues of diabetic WT mice. Hierarchical clustering identified 33 genes that were significantly upregulated only in diabetic WT mice but not remarkably changed in nondiabetic WT mice, nondiabetic ICAM-$1^{-/-}$ mice, or diabetic ICAM-$1^{-/-}$ mice (cluster 4; Fig. 1*A*). We focused on CCK because CCK is one of the most upregulated genes in cluster 4. Real-time RT-PCR revealed that the expression of CCK mRNA in the kidney cortices was significantly higher in diabetic WT mice

group compared with the diabetic WT group. Fifteen randomly selected glomeruli per mouse were examined (n = 4/group). *P < 0.05; ***P < 0.001. *G*: Expression of WT-1 in glomeruli. *H*: The average number of WT-1–positive cells in glomeruli. Podocyte loss was significantly increased in diabetic CCK-1R$^{-/-}$,-2R$^{-/-}$ mice as compared with the other three groups. Twenty randomly selected glomeruli per mouse were examined (n = 4/group). Values are the means ± SEM. **P < 0.01; ***P < 0.001. Scale bars, 50 μm. *I–L*: Expression of CCK and proinflammatory genes in the renal cortex. Expression of CCK was significantly increased to similar levels in both diabetic groups compared with the nondiabetic groups, whereas the expressions of CCL2, ICAM-1, and CD68 were significantly upregulated only in the diabetic CCK-1R$^{-/-}$,-2R$^{-/-}$ group (n = 6/group). Values are presented as ratio of nondiabetic WT. Results (mean ± SEM) are representative of three independent experiments. *M*: Expression of KIM-1 gene in the kidney. Expression of KIM-1 was significantly increased in diabetic CCK-1R$^{-/-}$,-2R$^{-/-}$ mice as compared with the other three groups (n = 6/group). Values are presented as the ratio of nondiabetic WT. Results (mean ± SEM) are representative of three independent experiments. *N*: Time course of UACR after induction of diabetes. The UACR of WT mice that received a bone marrow transplant from CCK-1 receptor-deficient mice (1R$^{-/-}$ →WT; ◆) was markedly increased after induction of diabetes as compared with that of other groups. WT→WT (●), WT mice that received a BMT from WT mice; WT→1R$^{-/-}$ (◇), CCK-1 receptor-deficient mice that received a BMT from WT mice. Values are the means ± SEM. *P < 0.05 vs. other groups. (A high-quality digital representation of this figure is available in the online issue.)

than in diabetic ICAM-1$^{-/-}$ mice (Fig. 1*B*), whereas there was no difference in CCK-1R or CCK-2R mRNA expression (Fig. 1*C* and *D*). We confirmed the distribution of CCK in the kidney tissues by immunoperoxidase staining. CCK was widely distributed in kidney tissues of nondiabetic WT mouse (Fig. 1*E–G*). In diabetic WT mice, the distal tubules and glomeruli were stained more intensely than in nondiabetic WT mice (Fig. 1*H–J*).

Diabetic CCK-1R$^{-/-}$,-2R$^{-/-}$ mice exhibited increased albuminuria with upregulated proinflammatory genes in the kidney. At 3 months after induction of diabetes, there was no significant difference in A1C, body weights, and creatinine clearance between the diabetic WT and diabetic CCK-1R$^{-/-}$,-2R$^{-/-}$ groups (Table 1). Kidney weight per body weight was increased not only in the diabetic WT and diabetic CCK-1R$^{-/-}$,-2R$^{-/-}$ groups but also in the nondiabetic CCK-1R$^{-/-}$,-2R$^{-/-}$ group (Table 1). It was noteworthy that the urinary albumin/creatinine ratio was markedly increased in diabetic CCK-1R$^{-/-}$,-2R$^{-/-}$ mice from 1 month to the end of the observation period compared with the diabetic WT mice (Fig. 2*A*). Furthermore, we compared levels of albuminuria among diabetic WT, CCK-1R$^{-/-}$, CCK-2R$^{-/-}$, and CCK-1R$^{-/-}$,-2R$^{-/-}$ mice. Although there was no statistical significance, CCK-1R$^{-/-}$,-2R$^{-/-}$ mice exhibited the most increased albuminuria at 3 months (Fig. 2*A*). Representative findings of the glomeruli in PAM-stained sections are shown in Fig. 2*B*. Glomerular hypertrophy was observed in both diabetic groups compared with the nondiabetic WT group at the end of the 3-month observation period (Fig. 2*C*). Mesangial matrix expansion was observed in both diabetic groups, but was more prominent in the diabetic CCK-1R$^{-/-}$,-2R$^{-/-}$ group than in the diabetic WT group (Fig. 2*D*). Type IV collagen intensity was higher in both diabetic groups than nondiabetic groups, and the intensity in the diabetic CCK-1R$^{-/-}$,-2R$^{-/-}$ group was further increased as compared with that in the diabetic WT group (Fig. 2*E* and *F*). Immunoperoxidase staining of WT-1, a normal podocyte marker, was performed to investigate the effect of CCK-8S in the progression of podocyte loss (Fig. 2*G*). The number of WT-1–positive cells per glomerulus was significantly decreased in the diabetic WT and both CCK-1R$^{-/-}$,-2R$^{-/-}$ groups, whereas podocyte loss was more prominent in the diabetic CCK-1R$^{-/-}$,-2R$^{-/-}$ group (Fig. 2*H*). CCK mRNA expression in the renal cortex was increased to the same extent in the diabetic WT group and diabetic CCK-1R$^{-/-}$,-2R$^{-/-}$ group compared with the nondiabetic groups (Fig. 2*I*). In contrast, mRNA of CCL2, ICAM-1, cluster of differentiation (CD) 68, and kidney injury molecule-1 (KIM-1; a marker of tubular damage) were significantly upregulated in the diabetic CCK-1R$^{-/-}$,-2R$^{-/-}$ group compared with the diabetic WT group (Fig. 2*J–M*). These findings suggest that diabetic renal injuries were exacerbated by deletion of both CCK-1R and CCK-2R via the inflammatory process. Furthermore, we performed BMT study to clarify whether deficiency of CCK-1R on infiltrating macrophages or resident renal cells is more important for the exacerbation of diabetic renal injury. BMT study showed that 1R$^{-/-}$→WT mice exhibited significantly increased relative kidney weight (Supplementary Table 3) and albuminuria (Fig. 2*N*) compared with WT→1R$^{-/-}$ and WT→WT mice, suggesting the importance of CCK-1R on macrophages.

Distribution of CCK in rat renal tissues. In the renal cortex of adult rats, the distribution of CCK was comparatively localized in distal tubules and glomeruli (Fig. 3*A* and *B*). In the renal medulla, the collecting ducts were stained intensely (Fig. 3*C*). We also identified CCK mRNA expression by real-time RT-PCR in the kidney cortex and isolated glomeruli obtained from normal adult rats (Fig. 3*E*).

CCK-8S ameliorates urinary albumin excretion and inhibits both macrophage infiltration and podocyte loss in glomeruli. At 8 weeks after induction of diabetes, systolic blood pressure, A1C, and kidney weight per body weight were elevated to the same level in both diabetic groups. However, there was no significant difference between DM and DM-CCK (Table 2). The body weight and serum creatinine of both diabetic groups were lower than that of the NDM animals. However, there was no significant difference between the DM and DM-CCK groups (Table 2). Fasting serum CCK levels in the DM-CCK group was increased ~3.9-fold than that of the DM group (514 ± 89 vs. 132 ± 33 pg/mL).

It is noteworthy that CCK-8S treatment significantly reduced urinary albumin excretion compared with the DM group at 8 weeks (Fig. 4*A*). Food intake was increased to the same extent in both diabetic groups compared with the NDM group after induction of diabetes (Fig. 4*B*). Glomerular hypertrophy was observed in both diabetic groups as compared with the NDM group. There was no significant difference in glomerular size between the DM and DM-CCK groups (Fig. 4*C* and *D*). Mesangial matrix expansion was observed in the DM group; however, CCK-8S treatment significantly reduced mesangial matrix expansion compared with DM (Fig. 4*E*). Type IV collagen intensity was higher in the DM than the NDM group. CCK-8S treatment markedly reduced type IV collagen intensity compared with the DM animals (Fig. 4*F* and *G*). The average number of macrophages (ED1-positive cells) per glomerulus was markedly increased in the DM compared with the NDM group, whereas macrophage infiltration was significantly inhibited by CCK-8S treatment (Fig. 4*H* and *I*). The number of WT-1–positive cells per glomerulus was significantly decreased in the DM, whereas podocyte loss was significantly inhibited by CCK-8S treatment (Fig. 4*J* and *K*).

CCK-8S inhibits expression of proinflammatory genes and NF-κB activation in diabetic kidney. The mRNA expressions of CD68, ICAM-1, and TGF-β in the renal cortex were significantly upregulated in the DM group, and these increases were significantly suppressed by CCK-8S treatment (Fig. 5*A–C*). The increase of KIM-1 mRNA expression in the kidney of DM group was partially but significantly suppressed by CCK-8S treatment (Fig. 5*E*). In isolated glomeruli, CCK-8S treatment also decreased the

TABLE 2
Metabolic characteristics of untreated rats and CCK-8S–treated rats (8 weeks after induction of diabetes)

	NDM	DM	DM-CCK
n	7	7	7
SBP, mmHg	114.0 ± 3.6	128.5 ± 1.4*	123.9 ± 1.4*
BW, g	485.5 ± 11.5	266.3 ± 22.4†	301.7 ± 11.2†
Kidney weight, mg/g BW	5.3 ± 0.1	10.0 ± 0.3†	10.5 ± 0.3†
A1C, %	3.7 ± 0.1	11.6 ± 0.6†	11.0 ± 0.5†
Cr, mg/dL	0.30 ± 0.01	0.21 ± 0.02*	0.16 ± 0.02†
Ccr, mL · min^{-1} · g BW^{-1}	7.8 ± 0.4	9.9 ± 1.2	10.0 ± 0.6

Data are means ± SEM. BW, body weight; Ccr, creatinine clearance; Cr, creatinine. *$P < 0.05$ vs. NDM. †$P < 0.001$ vs. NDM.

mRNA expressions of CD68, ICAM-1, TGF-β, and TNF-α as compared with DM (Fig. 5*F–I*). Interestingly, CCK-8S treatment markedly increased the mRNA expression of nephrin in glomeruli as compared with DM (Fig. 5*J*). These findings suggest that CCK-8S inhibits the development of albuminuria via inhibition of proinflammatory genes in the diabetic kidney. NF-κB p65-dependent DNA-binding activity in the renal cortex was significantly increased in the DM compared with the NDM group. CCK-8S treatment significantly decreased the NF-κB p65-dependent DNA-binding activity (Fig. 5*K*).

CCK-8S suppresses TNF-α expression and chemotaxis in THP-1 cells. TNF-α mRNA expression was significantly increased in the untreated HG group (Fig. 6*A*). Although TNF-α mRNA expression was not suppressed in the scrambled peptide-treated HG group, it was suppressed in the CCK-8S–treated (10^{-6} M) HG group compared with the untreated HG group (Fig. 6*A*). In addition, the anti-inflammatory effect of CCK-8S was largely abrogated by proglumide (an antagonist for both CCK receptors) (Fig. 6*A*). The number of THP-1 cells migrated into the lower chamber of the transwell was significantly reduced by CCK-8S treatment in a dose-dependent manner and was not reduced by scrambled peptide. These antimigratory effects of CCK-8S were completely abolished by proglumide (Fig. 6*B*).

DISCUSSION

In present study, we found that CCK is one of the significantly upregulated genes in the diabetic WT kidney compared with the diabetic ICAM-$1^{-/-}$ kidney. We hypothesized that CCK might regulate inflammatory response in the diabetic kidney; however, little is known about the role of CCK and its receptors in the development of diabetic nephropathy.

Two types of CCK receptors have been identified (27,28). These receptors have been classified as CCK-1R and CCK-2R based on their highly distinctive ligand selectivities (18). The two types of CCK receptors are distributed in various cells or tissues, including the kidneys (29–33) and macrophages (34,35). CCK-$1R^{-/-}$,-$2R^{-/-}$ mice are fertile and show no apparent developmental defects. It has been reported that the weights of the kidneys and liver are significantly increased in CCK-$1R^{-/-}$,-$2R^{-/-}$ mice compared with WT mice, although no abnormality is visible in these organs (17). In this study, deletion of both CCK-1R and CCK-2R enhanced inflammatory reactions and exacerbated the development of albuminuria after induction of diabetes. Our results suggest that CCK is increased in the diabetic kidney of mice and may regulate macrophage-related proinflammatory genes via CCK receptors. Furthermore, BMT study revealed that CCK-1R on macrophages played a more important role in the early stage of diabetic nephropathy than CCK-1R on resident renal cells. In the BMT study, we used CCK-$1R^{-/-}$ mice, because CCK-1R on macrophages plays a more dominant role in the anti-inflammatory effect of CCK-8S than CCK-2R (12). In contrast, CCK-2R is expressed on renal cells including murine mesangial cells (32). And the systemic absence of CCK-2R also exacerbated the development of albuminuria after induction of diabetes almost same extent as in CCK-$1R^{-/-}$ mice. Therefore, although further BMT study is needed, endogenous CCK might act against not only infiltrating macrophages but also resident renal cells via CCK-2R.

Several transcription factors have been implicated in the glucose-mediated expression of genes involved in diabetic nephropathy (36). NF-κB is one of the key mediators in the inflammatory response and plays a pivotal role in the progression of diabetic nephropathy (37). Activation of NF-κB in both kidney tissues obtained by biopsies and human peripheral blood mononuclear cells has been shown to correlate with degree of diabetic nephropathy (38,39). And NF-κB is also involved in regulation of ICAM-1 expression in diabetic kidney (36). Li et al. (12) reported that CCK-8S inhibited lipopolysaccharide-induced cytokine production via suppression of NF-κB activity. We showed that CCK-8S significantly suppressed NF-κB activation in the diabetic kidney, suggesting that CCK-8S may inhibit ICAM-1 expression via inhibition of NF-κB activity and thus lead to suppression of macrophage infiltration in the diabetic kidney.

Guha et al. (40) reported that high glucose-induced TNF-α mRNA expression in THP-1 cells was mediated by NF-κB. Our results indicate that inhibition of both high glucose-induced TNF-α expression via NF-κB and CCL2-induced migration might be involved in the anti-inflammatory effects of CCK-8S in THP-1 cells. Because the nephrin gene expression in cultured podocyte is repressed by TNF-α at a transcriptional level (41), our results suggest that CCK-8S may prevent podocyte loss via inhibition of TNF-α mRNA expression in diabetic glomeruli.

Aunapuu et al. (42) recently reported that CCK overexpression was associated with renal morphological damage in transgenic mice without a significant difference in kidney weight or proteinuria, but with a thickened glomerular basement membrane. CCK is expressed from embryonic day (E) 8.5, whereas both CCK-1R and CCK-2R have been identified from E10.5; in addition, CCK is thought to affect tissue growth and differentiation (43). In another study, both CCK-1R and CCK-2R expression were confirmed from E14.5 in kidney tissues (33), and therefore, CCK might regulate renal microstructural growth. In nondiabetic CCK-$1R^{-/-}$,-$2R^{-/-}$ mice, increased kidney and liver weight (17) and reduction in the number of glomerular podocytes also suggest that CCK may play a role in regulating the development or growth of these organs. In the current study, we examined the effect of CCK-8S using an STZ-induced diabetic model, but no nephrotoxicity was observed.

Because the half-time of CCK-8S in blood is short, it would be difficult to use a longer period for maintaining renoprotective effect in patients with diabetic nephropathy. Recently, León-Tamariz et al. (44) reported that PEGylated CCK-10, which did not cross the blood-brain barrier, maintained blood concentration longer than free CCK. Such drugs with a longer duration of action may be more suitable for clinical use.

In conclusion, we have shown that CCK is expressed in the kidney, and deficiency of both CCK-1R and CCK-2R accelerates development of albuminuria by enhancement of inflammation in the kidneys after induction of diabetes. Administration of CCK-8S confers protection against renal inflammation, leading to a reduction of albuminuria in diabetic rats. Furthermore, CCK-8S directly inhibits high glucose-induced TNF-α expression and migration in cultured THP-1 cells. Our findings may provide a novel strategy of therapy for the early stage of diabetic nephropathy and other inflammatory diseases.

ACKNOWLEDGMENTS

This study was supported in part by Grants-in-Aid for Scientific Research from the Ministry of Education, Science,

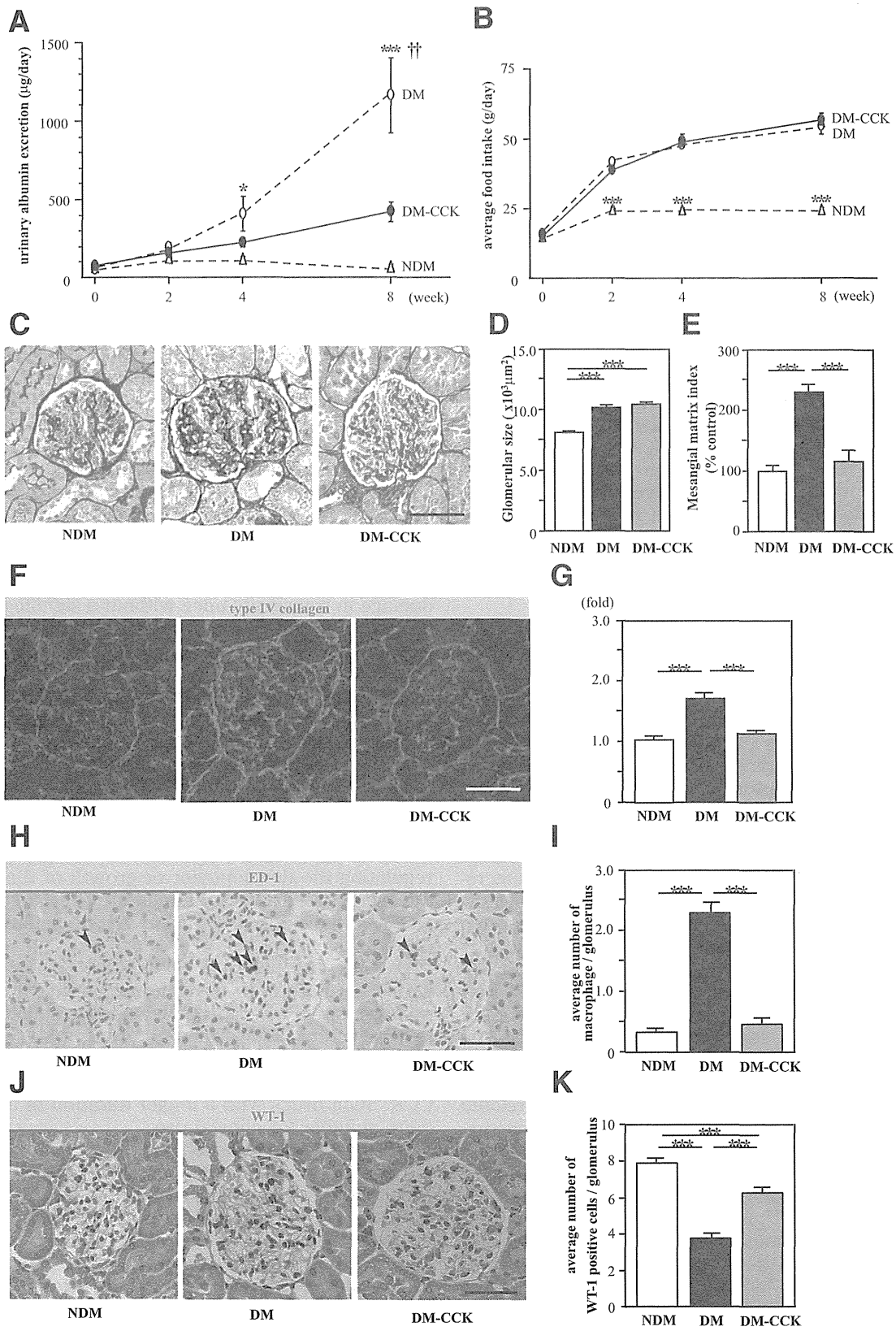

FIG. 4. CCK-8S ameliorates urinary albumin excretion and inhibits macrophage infiltration in glomeruli. *A*: Time course of urinary albumin excretion (UAE). The UAE of untreated diabetic rats (DM; ○) was increased progressively compared with that in nondiabetic rats (NDM; △), whereas it was suppressed in CCK-8S–treated diabetic rats (DM-CCK; ●) at week 8 (n = 7/group). Values are the means ± SEM. *P < 0.05 vs. NDM; ***P < 0.001 vs. NDM; ††P < 0.01 vs. DM-CCK. *B*: There was no difference in the amount of food intake between DM (○) and DM-CCK (●). ***P < 0.001 vs. DM and DM-CCK. Values are the means ± SEM. *C*: PAM staining of the kidney at 8 weeks. *D*: Glomerular hypertrophy was observed in both diabetic groups as compared with nondiabetic rats. Values are the means ± SEM. ***P < 0.001. *E*: Mesangial matrix index was ameliorated in CCK-8S–treated diabetic rats compared with untreated diabetic rats. Values are the means ± SEM. ***P < 0.001. Fifteen randomly selected glomeruli per rat were examined (n = 5/group). *F*: Expression of type IV collagen in kidney tissue. *G*: Type IV collagen-positive area in glomeruli

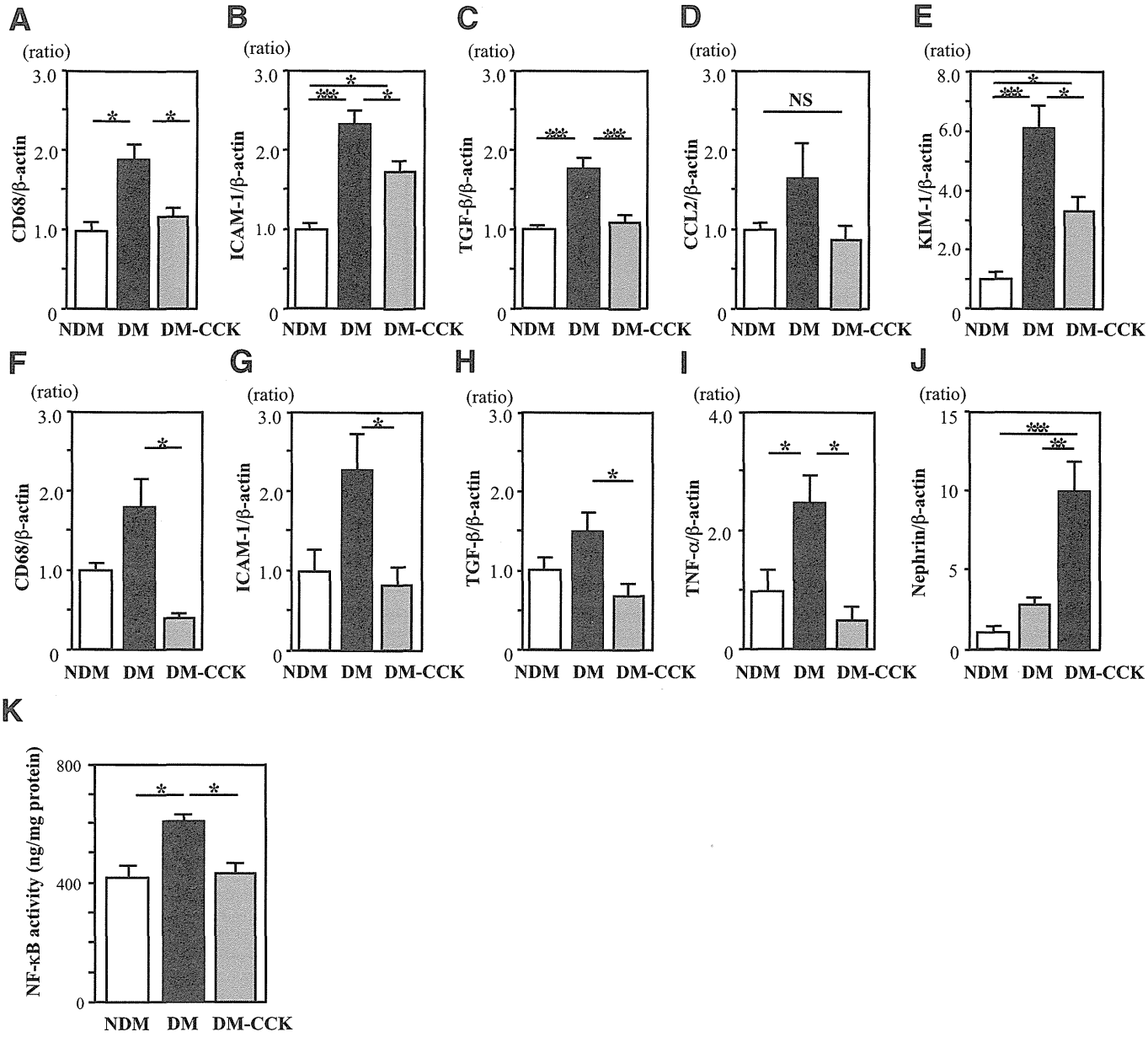

FIG. 5. CCK-8S inhibits expression of proinflammatory genes and NF-κB p65-dependent DNA-binding activity in the kidney of diabetic rats. *A–D*: Expression of proinflammatory genes in the renal cortex. CCK-8S treatment significantly decreased the mRNA levels of CD68 (*A*), ICAM-1 (*B*), and TGF-β (*C*) in the renal cortex as compared with those in untreated diabetic rats (n = 6/group). *E*: Expression of KIM-1 gene in the kidney was significantly inhibited by CCK-8S treatment. *F–I*: Expression of proinflammatory and nephrin genes in the isolated glomeruli (n = 4/group). CCK-8S treatment was significantly decreased the mRNA level of CD68 (*F*), ICAM-1 (*G*), TGF-β (*H*), and TNF-α (*I*) in isolated glomeruli as compared with untreated diabetic rats. In contrast, CCK-8S treatment was significantly increased the mRNA level of nephrin (*J*) in isolated glomeruli as compared with untreated diabetic rats. Values (means ± SEM) are presented as the ratio of NDM. *P < 0.05; **P < 0.01; ***P < 0.001; NS, P > 0.05. *K*: CCK-8S treatment ameliorates diabetes-induced NF-κB p65-dependent DNA-binding activity in the nuclear extracts of the rat kidney cortex (n = 6/group). *P < 0.05. Results (means ± SEM) are representative of two to three independent experiments.

Culture, Sports and Technology of Japan (Grant 21591031 to K.S.) and the Ministry of Health, Labour and Welfare of Japan.

No potential conflicts of interest relevant to this article were reported.

S.M. researched data, contributed to discussion, and wrote the manuscript. K.S. contributed to discussion and reviewed and edited the manuscript. K.M. researched data and reviewed and edited the manuscript. S.O., M.S., R.K.,

(folds versus NDM). Type IV collagen was significantly increased in the DM compared with the DM-CCK group. Fifteen randomly selected glomeruli per rat were examined (n = 4/group). Values are the means ± SEM. ***P < 0.001. *H*: Macrophage infiltration into glomeruli at 8 weeks. Arrowheads indicate macrophages. *I*: The average number of intraglomerular macrophages. Macrophage infiltration into glomeruli was remarkable in the DM, whereas it was minimal in the DM-CCK group. Twenty randomly selected glomeruli per rat were examined (n = 4/group). Values are the means ± SEM. ***P < 0.001. *J*: Expression of WT-1 in glomeruli. *K*: The average number of WT-1–positive cells in glomeruli. Podocyte loss was inhibited in CCK-8S–treated diabetic rats compared with untreated diabetic rats. Twenty randomly selected glomeruli per rat were examined (n = 4/group). Values are the means ± SEM. ***P < 0.001. Scale bars, 50 μm. (A high-quality digital representation of this figure is available in the online issue.)

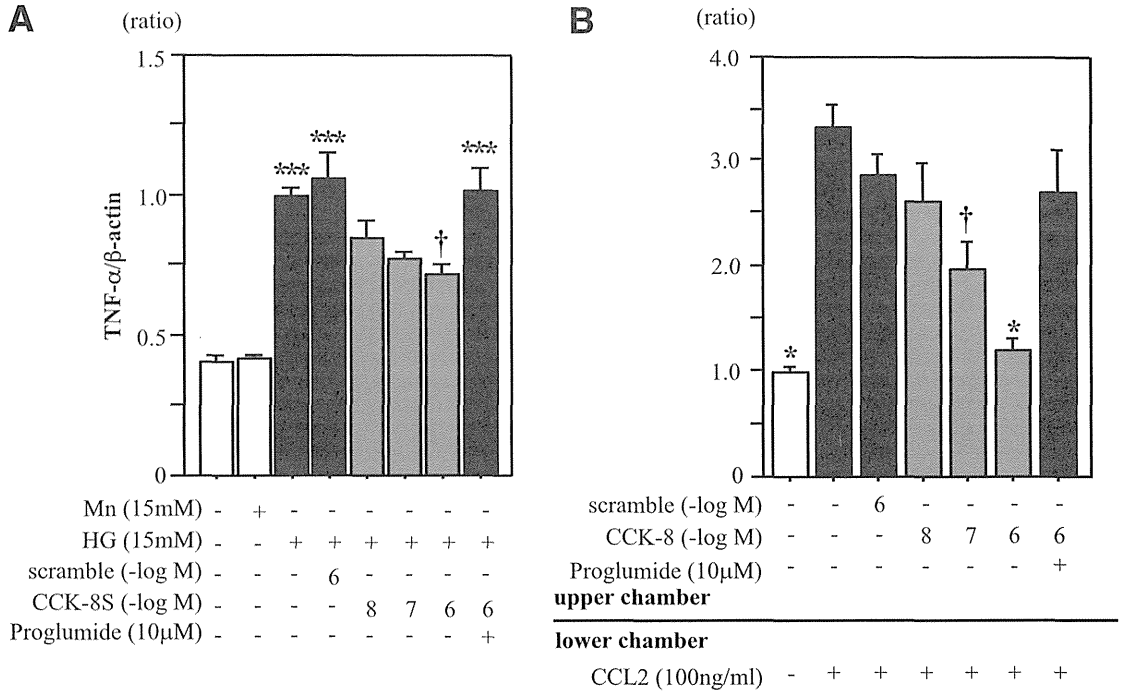

FIG. 6. CCK-8S suppresses both expression of TNF-α and chemotaxis in THP-1 cells. *A*: THP-1 cells were cultured under different conditions for 72 h. CCK-8S inhibited HG-induced TNF-α expression in THP-1 cells (n = 5 each). Values are presented as the ratio of HG group. ***P < 0.001 vs. the NG and Mn groups; †P < 0.05 vs. the HG, scrambled peptide, and proglumide (a nonselective CCK receptor antagonist) groups. *B*: CCK-8S blocks the CCL2-induced chemotaxis in THP-1 cells (n = 5 per group). Values are presented as the ratio of untreated group. *P < 0.05 vs. the CCL2, CCL2 with scrambled peptide, and CCL2 with proglumide groups; †P < 0.05 vs. the CCL2 group. Results (means ± SEM) are representative of two to three independent experiments.

D.H., N.K., T.T., S.N., C.S., A.F., H.N., and H.A.U. researched data. H.U.K., D.O., and H.M. contributed to discussion. K.S. is the guarantor of this work and, as such, had full access to all the data in the study and takes responsibility for the integrity of the data and the accuracy of the data analysis.

REFERENCES

1. Ritz E, Rychlík I, Locatelli F, Halimi S. End-stage renal failure in type 2 diabetes: A medical catastrophe of worldwide dimensions. Am J Kidney Dis 1999;34:795–808
2. Adler AI, Stevens RJ, Manley SE, Bilous RW, Cull CA, Holman RR; UKPDS GROUP. Development and progression of nephropathy in type 2 diabetes: the United Kingdom Prospective Diabetes Study (UKPDS 64). Kidney Int 2003;63:225–232
3. Nelson CL, Karschimkus CS, Dragicevic G, et al. Systemic and vascular inflammation is elevated in early IgA and type 1 diabetic nephropathies and relates to vascular disease risk factors and renal function. Nephrol Dial Transplant 2005;20:2420–2426
4. Sugimoto H, Shikata K, Hirata K, et al. Increased expression of intercellular adhesion molecule-1 (ICAM-1) in diabetic rat glomeruli: glomerular hyperfiltration is a potential mechanism of ICAM-1 upregulation. Diabetes 1997;46:2075–2081
5. Okada S, Shikata K, Matsuda M, et al. Intercellular adhesion molecule-1-deficient mice are resistant against renal injury after induction of diabetes. Diabetes 2003;52:2586–2593
6. Jorpes E, Mutt V. Cholecystokinin and pancreozymin, one single hormone? Acta Physiol Scand 1966;66:196–202
7. Mutt V, Jorpes JE. Structure of porcine cholecystokinin-pancreozymin. 1. Cleavage with thrombin and with trypsin. Eur J Biochem 1968;6:156–162
8. Dufresne M, Seva C, Fourmy D. Cholecystokinin and gastrin receptors. Physiol Rev 2006;86:805–847
9. Rehfeld JF. Clinical endocrinology and metabolism. Cholecystokinin. Best Pract Res Clin Endocrinol Metab 2004;18:569–586
10. Crawley JN, Corwin RL. Biological actions of cholecystokinin. Peptides 1994;15:731–755
11. Meng AH, Ling YL, Zhang XP, Zhang JL. Anti-inflammatory effect of cholecystokinin and its signal transduction mechanism in endotoxic shock rat. World J Gastroenterol 2002;8:712–717
12. Li S, Ni Z, Cong B, et al. CCK-8 inhibits LPS-induced IL-1beta production in pulmonary interstitial macrophages by modulating PKA, p38, and NF-kappaB pathway. Shock 2007;27:678–686
13. Bozkurt A, Cakir B, Ercan F, Yeğen BC. Anti-inflammatory effects of leptin and cholecystokinin on acetic acid-induced colitis in rats: role of capsaicin-sensitive vagal afferent fibers. Regul Pept 2003;116:109–118
14. Luyer MD, Greve JW, Hadfoune M, Jacobs JA, Dejong CH, Buurman WA. Nutritional stimulation of cholecystokinin receptors inhibits inflammation via the vagus nerve. J Exp Med 2005;202:1023–1029
15. Sligh JE Jr, Ballantyne CM, Rich SS, et al. Inflammatory and immune responses are impaired in mice deficient in intercellular adhesion molecule 1. Proc Natl Acad Sci USA 1993;90:8529–8533
16. Usui HK, Shikata K, Sasaki M, et al. Macrophage scavenger receptor-a-deficient mice are resistant against diabetic nephropathy through amelioration of microinflammation. [Published erratum appears in Diabetes 2007; 56:897.] Diabetes 2007;56:363–372
17. Miyasaka K, Ichikawa M, Ohta M, et al. Energy metabolism and turnover are increased in mice lacking the cholecystokinin-B receptor. J Nutr 2002; 132:739–741
18. Takiguchi S, Suzuki S, Sato Y, et al. Role of CCK-A receptor for pancreatic function in mice: a study in CCK-A receptor knockout mice. Pancreas 2002;24:276–283
19. Nagata A, Ito M, Iwata N, et al. G protein-coupled cholecystokinin-B/gastrin receptors are responsible for physiological cell growth of the stomach mucosa in vivo. Proc Natl Acad Sci USA 1996;93:11825–11830
20. Asakura S, Hashimoto D, Takashima S, et al. Alloantigen expression on non-hematopoietic cells reduces graft-versus-leukemia effects in mice. J Clin Invest 2010;120:2370–2378
21. Nishimori H, Maeda Y, Teshima T, et al. Synthetic retinoid Am80 ameliorates chronic graft-versus-host disease by downregulating Th1 and Th17. Blood 2012;119:285–295
22. Uchida HA, Poduri A, Subramanian V, Cassis LA, Daugherty A. Urokinase-type plasminogen activator deficiency in bone marrow-derived cells augments rupture of angiotensin II-induced abdominal aortic aneurysms. Arterioscler Thromb Vasc Biol 2011;31:2845–2852

23. Fong JS, Drummond KN. Method for preparation of glomeruli for metabolic studies. J Lab Clin Med 1968;71:1034–1039
24. Kodera R, Shikata K, Kataoka HU, et al. Glucagon-like peptide-1 receptor agonist ameliorates renal injury through its anti-inflammatory action without lowering blood glucose level in a rat model of type 1 diabetes. Diabetologia 2011;54:965–978
25. Wågsäter D, Zhu C, Björck HM, Eriksson P. Effects of PDGF-C and PDGF-D on monocyte migration and MMP-2 and MMP-9 expression. Atherosclerosis 2009;202:415–423
26. Gómez-Garre D, Muñoz-Pacheco P, González-Rubio ML, Aragoncillo P, Granados R, Fernández-Cruz A. Ezetimibe reduces plaque inflammation in a rabbit model of atherosclerosis and inhibits monocyte migration in addition to its lipid-lowering effect. Br J Pharmacol 2009;156:1218–1227
27. Wank SA, Harkins R, Jensen RT, Shapira H, de Weerth A, Slattery T. Purification, molecular cloning, and functional expression of the cholecystokinin receptor from rat pancreas. Proc Natl Acad Sci USA 1992;89:3125–3129
28. Kopin AS, Lee YM, McBride EW, et al. Expression cloning and characterization of the canine parietal cell gastrin receptor. Proc Natl Acad Sci USA 1992;89:3605–3609
29. Lacourse KA, Lay JM, Swanberg LJ, Jenkins C, Samuelson LC. Molecular structure of the mouse CCK-A receptor gene. Biochem Biophys Res Commun 1997;236:630–635
30. Galindo J, Jones N, Powell GL, Hollingsworth SJ, Shankley N. Advanced qRT-PCR technology allows detection of the cholecystokinin 1 receptor (CCK1R) expression in human pancreas. Pancreas 2005;31:325–331
31. von Schrenck T, Ahrens M, de Weerth A, et al. CCKB/gastrin receptors mediate changes in sodium and potassium absorption in the isolated perfused rat kidney. Kidney Int 2000;58:995–1003
32. de Weerth A, Jonas L, Schade R, et al. Gastrin/cholecystokinin type B receptors in the kidney: molecular, pharmacological, functional characterization, and localization. Eur J Clin Invest 1998;28:592–601
33. Lay JM, Jenkins C, Friis-Hansen L, Samuelson LC. Structure and developmental expression of the mouse CCK-B receptor gene. Biochem Biophys Res Commun 2000;272:837–842
34. Sacerdote P, Wiedermann CJ, Wahl LM, Pert CB, Ruff MR. Visualization of cholecystokinin receptors on a subset of human monocytes and in rat spleen. Peptides 1991;12:167–176
35. Xu SJ, Gao WJ, Cong B, Yao YX, Gu ZY. Effect of lipopolysaccharide on expression and characterization of cholecystokinin receptors in rat pulmonary interstitial macrophages. Acta Pharmacol Sin 2004;25:1347–1353
36. Sanchez AP, Sharma K. Transcription factors in the pathogenesis of diabetic nephropathy. Expert Rev Mol Med 2009;11:e13
37. Lee FT, Cao Z, Long DM, et al. Interactions between angiotensin II and NF-kappaB-dependent pathways in modulating macrophage infiltration in experimental diabetic nephropathy. J Am Soc Nephrol 2004;15:2139–2151
38. Nam JS, Cho MH, Lee GT, et al. The activation of NF-kappaB and AP-1 in peripheral blood mononuclear cells isolated from patients with diabetic nephropathy. Diabetes Res Clin Pract 2008;81:25–32
39. Hofmann MA, Schiekofer S, Isermann B, et al. Peripheral blood mononuclear cells isolated from patients with diabetic nephropathy show increased activation of the oxidative-stress sensitive transcription factor NF-kappaB. Diabetologia 1999;42:222–232
40. Guha M, Bai W, Nadler JL, Natarajan R. Molecular mechanisms of tumor necrosis factor alpha gene expression in monocytic cells via hyperglycemia-induced oxidant stress-dependent and -independent pathways. J Biol Chem 2000;275:17728–17739
41. Takano Y, Yamauchi K, Hayakawa K, et al. Transcriptional suppression of nephrin in podocytes by macrophages: roles of inflammatory cytokines and involvement of the PI3K/Akt pathway. FEBS Lett 2007;581:421–426
42. Aunapuu M, Roosaar P, Järveots T, et al. Altered renal morphology in transgenic mice with cholecystokinin overexpression. Transgenic Res 2008;17:1079–1089
43. Lay JM, Gillespie PJ, Samuelson LC. Murine prenatal expression of cholecystokinin in neural crest, enteric neurons, and enteroendocrine cells. Dev Dyn 1999;216:190–200
44. León-Tamariz F, Verbaeys I, Van Boven M, et al. Biodistribution and pharmacokinetics of PEG-10kDa-cholecystokinin-10 in rats after different routes of administration. Curr Drug Deliv 2010;7:137–143

Clin Exp Nephrol (2012) 16:739–748
DOI 10.1007/s10157-012-0625-3

ORIGINAL ARTICLE

Phenotypic change of macrophages in the progression of diabetic nephropathy; sialoadhesin-positive activated macrophages are increased in diabetic kidney

Ryo Nagase · Nobuo Kajitani · Kenichi Shikata · Daisuke Ogawa · Ryo Kodera · Shinichi Okada · Yuichi Kido · Hirofumi Makino

Received: 25 August 2011 / Accepted: 8 March 2012 / Published online: 14 April 2012

Abstract
Background Inflammatory process is involved in pathogenesis of diabetic nephropathy, although the activation and phenotypic change of macrophages in diabetic kidney has remained unclear. Sialoadhesin is a macrophage adhesion molecule containing 17 extracellular immunoglobulin-like domains, and is an I-type lectin which binds to sialic acid ligands expressed on hematopoietic cells. The aim of this study is to clarify the activation and phenotypic change of macrophages in the progression of diabetic nephropathy.
Methods We examined the expression of surface markers for pan-macrophages, resident macrophages, sialoadhesin, major histocompatibility complex class II and α-smooth muscle actin in the glomeruli of diabetic rats using immunohistochemistry at 0, 1, 4, 12, and 24 weeks after induction of diabetes by streptozotocin. Expression of type IV collagen and the change of mesangial matrix area were also measured. The mechanism for up-regulated expression of sialoadhesin on macrophages was evaluated in vitro.
Results The number of macrophages was increased in diabetic glomeruli at 1 month after induction of diabetes and the increased number was maintained until 6 months. On the other hand, sialoadhesin-positive macrophages were increased during the late stage of diabetes concomitantly with the increase of α-smooth muscle actin-positive mesangial cells, mesangial matrix area and type IV collagen. Gene expression of sialoadhesin was induced by stimulation with interleukin (IL)-1β and tumor necrosis factor-α but not with IL-4, transforming growth factor-β and high glucose in cultured human macrophages.
Conclusion The present findings suggest that sialoadhesin-positive macrophages may contribute to the progression of diabetic nephropathy.

Keywords Macrophage · Sialoadhesin · Diabetic nephropathy

R. Nagase and N. Kajitani contributed equally to this work.

R. Nagase · N. Kajitani · K. Shikata (✉) · D. Ogawa (✉) · R. Kodera · S. Okada · Y. Kido · H. Makino
Department of Medicine and Clinical Science, Okayama University Graduate School of Medicine, Dentistry and Pharmaceutical Sciences, 2-5-1 Shikata-cho, Kita-ku, Okayama 700-8558, Japan
e-mail: shikata@md.okayama-u.ac.jp

D. Ogawa
e-mail: daiogawa@md.okayama-u.ac.jp

K. Shikata · R. Kodera
Center for Innovative Clinical Medicine, Okayama University Hospital, Okayama, Japan

D. Ogawa
Department of Diabetic Nephropathy, Okayama University Graduate School of Medicine, Dentistry and Pharmaceutical Sciences, Okayama, Japan

Introduction

Diabetic nephropathy is a leading cause of end-stage renal failure in developed countries. Infiltration of mononuclear cells is a characteristic of the glomeruli in patients with diabetes [1]. We previously demonstrated that intercellular adhesion molecule-1 (ICAM-1) mediates macrophage infiltration into the glomeruli of streptozotocin (STZ)-induced diabetic rats [2]. Furthermore, we demonstrated that infiltration of macrophages was suppressed in diabetic ICAM-1 knockout mice and urinary albumin excretion, glomerular hypertrophy and mesangial matrix expansion were significantly suppressed in diabetic ICAM-1 knockout mice compared to diabetic wild-type mice [3]. These

findings strongly suggest the important role of macrophages in the progression of diabetic nephropathy, although the state of activation and the phenotype of macrophages infiltrated into diabetic glomeruli have remained unclear.

Sialoadhesin (Sn) is a sialic acid-dependent lectin-like receptor [4] which mediates cell to cell interactions. Expression of Sn is normally restricted to distinct subsets of tissue macrophages including lymphoid tissue macrophage [5]. Sn is induced rapidly in response to serum factors [6], glucocorticoids, and cytokines [7]. Recent studies in humans have shown that Sn is expressed abundantly on macrophages in the pathological tissues of multiple sclerosis, atherosclerosis, rheumatoid arthritis, and breast cancer [8], suggesting that Sn-positive macrophages are related to chronic inflammation.

Ito et al. [9] demonstrated that Sn-positive macrophages were observed in the prolonged model of mesangial proliferative glomerulonephritis. This study suggests that Sn-positive macrophages might be involved in chronic inflammation of the kidney. There have been some reports which describe the critical role of Sn-positive macrophages in the pathogenesis of experimental glomerulonephritis [10–12]; however, little is known about Sn-positive macrophages in the pathogenesis of diabetic nephropathy. To elucidate the relationship between Sn-positive macrophages and diabetic nephropathy, we analyzed the phenotypes of macrophages in diabetic glomeruli by immunohistochemically examining ED1 (pan-macrophages marker), ED2 (resident macrophages marker), and ED3 (Sn-positive macrophages marker) [13]. We also analyzed the activated macrophages which express OX-6 (major histocompatibility complex [MHC] class II-positive cell marker) on the cell surface.

Diabetic nephropathy is characterized histologically by glomerular hypertrophy, glomerular basement membrane thickening, mesangial matrix expansion, and ultimately glomerular sclerosis [14–17]. In diabetic glomerulosclerosis, there is an accumulation of matrix proteins, type IV collagen or fibronectin [18, 19]. Because the mesangial cells are responsible for this matrix protein synthesis, overproduction of these matrix proteins is considered to be a result of phenotypic change in the mesangial cells [18]. Therefore, we also analyzed α-smooth muscle actin (α-SMA) as a marker of the phenotypic change of mesangial cells [20, 21]. Furthermore, we examined the expression of ICAM-1, type IV collagen, and mesangial matrix area.

Materials and methods

Animals

Male Sprague–Dawley rats, weighing 120 g (4 weeks of age), were purchased from Charles River Japan (Yokohama, Japan) for use in this study. The rats received a standard chow and water diet. All procedures were performed according to the Guidelines for Animal Experiments at Okayama University Medical School, Japanese Government Animal Protection and Management Law (No. 105) and Japanese Government Notification on Feeding and Safekeeping of Animals (No. 6).

Induction of diabetes

Diabetes was induced in 25 rats by an intravenous injection of 65 mg/kg STZ (Sigma-Aldrich, St. Louis, MO, USA) in 10 mM citrate buffer solution (pH 4.5). The control rats were injected with citrate buffer alone. Blood was collected from a tail vein and assayed for glucose. Urinary protein was determined by the biuret method. Five diabetic and five control rats were sacrificed under anesthesia and the kidneys were harvested at 1, 4, 12, and 24 weeks after the STZ or buffer injection. Kidneys were weighed and fixed in 10 % formalin for periodic acid-methenamine silver (PAM) staining and the remaining tissues were embedded in Optimal Cutting Temperature (OCT) compound (Sakura Finetechnical Co., Tokyo, Japan) and immediately frozen in acetone cooled on dry ice. Metabolic data were measured as described previously [2].

Metabolic data

Blood glucose, urinary albumin excretion (24 h), and body weight were measured at 0, 1, 4, 12, and 24 weeks. Urine collection was performed for 24 h with each rat individually housed in a metabolic cage and having free access to food and water. Blood glucose was measured by the glucose oxidase method. Urinary albumin concentration was measured by nephelometry (Organon Teknika-Cappel, Durham, NC, USA). Glycosylated hemoglobin (HbA1c) was measured at 0, 1, 4, 12, and 24 weeks after induction of diabetes by latex agglutination assay.

Effect of insulin treatment

Three days after STZ administration, when all animals ($n = 5$) exhibited blood glucose levels >300 mg/dl, insulin treatment was initiated using nearly 24 h-acting Humalin N (Shionogi, Osaka, Japan) as described previously [2]. All insulin-treated rats were sacrificed at 4 weeks and processed for immunohistochemical studies.

Antibodies

As primary antibodies, we used mouse antibodies against rat pan-macrophages (ED1), resident macrophages (ED2), Sn-positive macrophages (ED3), and MHC class II-positive

cells (OX6); these antibodies were purchased from AbD Serotec (Oxford, UK). Mouse anti-rat ICAM-1 monoclonal antibody was purchased from Seikagaku Corporation (Tokyo, Japan). Rabbit anti-mouse collagen IV antibody was purchased from LSL (Tokyo, Japan). Mouse anti α-SMA monoclonal antibody was purchased from Oncogene (Boston, MA, USA).

As secondary antibodies, biotinylated goat anti-mouse immunoglobulin (Ig) G and fluorescein isothiocyanate (FITC)-labeled goat anti-mouse IgG were obtained from Jackson Immunoresearch Laboratories (West Grove, PA, USA). Rodamin-labeled anti-mouse IgG was obtained from Chemicon International (Temecula, CA, USA). FITC-labeled anti-rabbit IgG was obtained from Zymed Laboratories (San Francisco, CA, USA).

Histopathological examination

Immunoperoxidase and immunofluorescence staining were performed as described previously [2]. Fresh frozen sections were cut at 4-μm thickness using a cryostat. To evaluate the phenotype of infiltrated macrophages, anti-ED1, ED2, and ED3 antibodies were applied to the fresh frozen sections as the primary reaction, followed by a second reaction with rodamin-labeled anti-mouse IgG antibody. Then FITC-labeled anti-rat OX-6 antibody was double-stained. Intraglomerular ED1-, ED2-, ED3- and OX-6-positive cells were counted in 10 glomeruli from each animal (total 50 glomeruli for each group). The average number per glomerulus was used for estimation. ICAM-1 and type IV collagen were also detected by the indirect immunofluorescence method. Briefly, sections were fixed with cold acetone for 3 min and stained with each monoclonal antibody for 24 h at 4 °C. The sections were then stained with each FITC-labeled anti-IgG antibody for 30 min at room temperature. The sections were washed in phosphate buffered saline, mounted with PermaFluor (Shandon, Pittsburgh, PA, USA) and examined under a fluorescence microscope (LSM-510; Carl Zeiss, Jena, Germany). The intensity of ICAM-1 and type IV collagen in the glomeruli was evaluated semi-quantitatively from 0 to 3+.

The distribution of α-SMA was evaluated by immunoperoxidase assays using Vectastain (Vector, Burlingame, CA, USA). In brief, the frozen sections (4-μm thick) were fixed with cold acetone for 3 min and nonspecific protein binding was blocked by incubation with normal goat serum and avidin for 20 min. The sections were first incubated with each monoclonal antibody for 24 h at 4 °C. The sections were then incubated with biotin-labeled anti-IgG antibody for 30 min at room temperature. Endogenous peroxidase activity was blocked by incubating the sections in methanol containing 0.3 % hydrogen peroxide for 30 min; the sections were then stained with a Vectastain ABC kit and counterstained with Mayer's hematoxylin and the percentage of α-SMA-positive glomeruli was evaluated.

Light microscopy

Renal tissues were fixed in 10 % formalin and embedded in paraffin in a routine fashion. Tissue sections were cut at 4-μm thickness, dewaxed and stained with PAM. To evaluate glomerular size, 5 randomly selected glomeruli from the cortex of each animal were examined under high magnification (200×). The mesangial matrix area was defined as the PAM-positive area within the tuft area and was measured using Photoshop software Ver. 6 (Adobe Systems, San Jose, CA, USA) and analyzed by Scion Image Ver.4.0.2. The results are expressed as mean ± SEM (μm^2).

Cell culture

The human monocytic cell line THP-1 (Japanese Collection of Research Bioresources, Tokyo, Japan) was cultured in RPMI-1640 (Gibco-Invitrogen, Carlsbad, CA, USA) supplemented with heat-inactivated 10 % (v/v) fetal bovine serum (Thermo-Fisher Scientific, Waltham, MA, USA). Cells were cultured at 37 °C in humidified air containing 5 % carbon dioxide. For experiments, the cells were adjusted to the cell density of 10^6 cells/ml in the same culture medium. Cells were stimulated with recombinant human tumor necrosis factor-α (TNF-α; 0.01−10 μg/l) (R&D Systems, Minneapolis, MN, USA), recombinant human IL-1β (0.01−10 μg/l) (R&D Systems), recombinant human IL-4 (10 μg/l) (R&D Systems) and recombinant human transforming growth factor-β1 (TGF-β1; 10 μg/l) (R&D Systems). Cells were also stimulated under hyperglycemic conditions (5.4 g/l D-glucose) (Sigma-Aldrich); as an osmotic control, D-Mannitol (3.63 g/l) (Sigma-Aldrich) was added to culture medium in simultaneous wells. Total RNA was extracted from THP-1 cells 24 h after stimulation.

RNA extraction and quantitative real-time reverse transcription-polymerase chain reaction (RT-PCR)

Total RNA was extracted using the RNeasy Plus Mini Kit (Qiagen, Valencia, CA, USA) according to the manufacturer's instructions. Single-strand complementary DNA was synthesized from the extracted RNA using a GeneAmp RNA PCR Core kit (Applied Biosystems, Foster City, CA, USA) according to the manufacturer's instructions. To evaluate mRNA expression of Sn in THP-1 cells, and IL-1β and TNF-α in rat kidney, quantitative real-time RT-PCR was performed using a Light Cycler (Roche Diagnostics, Tokyo, Japan) and SYBR Premix Ex Taq II (Takara Bio,

Shiga, Japan) as previously described [22]. The mRNA expression was normalized with a house-keeping gene (*GAPDH* or β-actin) in each sample by calculating the relative expression ratio. For amplification of the complementary DNA, the following oligonucleotide primers were purchased from Takara Bio: Sn, sense 5′-CTGCGAAT CAGGGACCAACA-3′, antisense 5′-TTTCAACCCAAA TCCTAGAGCAGAG-3′; IL-1β, sense 5′-GCTGTGGCAG CTACCTATGTCTTG-3′, antisense 5′-AGGTCGTCATC ATCCCACGAG-3′; TNF-α, sense 5′-TCAGTTCCATG GCCCAGAC-3′, antisense 5′-GTTGTCTTTGAGATCCA TGCCATT-′; GAPDH, sense 5′-GCACCGTCAAGGCT-GAGAAC-3′, antisense 5′-TGGTGAAGACGCCAGTGG A-3′; β-actin, sense 5′-GGAGATTACTGCCCTGGCTCC TA-3′, antisense 5′-GACTCATCGTACTCCTGCTTGCT G-3′. Each experiment was performed twice.

Statistical analysis

All values are expressed as the mean ± SEM. Differences between groups were examined for statistical significance using one-way analysis of variance (ANOVA) followed by Scheffe's test. A P value <0.05 denoted the presence of a statistically significant difference.

Results

Metabolic data

Body weight, kidney weight, urinary albumin excretion, and glycosylated hemoglobin are shown in Table 1. Diabetic rats had a significantly lower body weight and higher kidney weight per body weight from 4 weeks after induction of diabetes. An increase in urinary albumin excretion was observed after 4 weeks. All diabetic rats were moderately hyperglycemic. The serum HbA1c concentration in the diabetic group was significantly higher than in the control group.

Phenotype of macrophage in the glomeruli

Throughout the experiment, ED1-, ED2-, ED3- and OX-6-positive macrophages were analyzed in the glomeruli of control rats and of animals with STZ-induced diabetes (Fig. 1). When the sections were incubated with irrelevant mouse IgG, no staining was observed. The glomeruli of control rats showed only a few ED1-, ED2-, and ED3-positive macrophages. In the rats with STZ-induced diabetes, ED1, which is expressed in pan macrophage, peaked at 1 week and maintained to 24 weeks; most of these macrophages were positive for MHC class II (OX-6) in the glomeruli. ED2, which is expressed in resident macrophage, was not increased in diabetic glomeruli. Sn-positive macrophage (ED3-positive) continued to increase gradually and most of these macrophages were also positive for MHC class II in the glomeruli (Fig. 1).

Expression of ICAM-1

In normal rat glomeruli, ICAM-1 staining was weakly detected. In the glomeruli of STZ-induced diabetes, ICAM-1 fluorescence intensity increased early after diabetes induction, reaching a peak at 12 weeks and was significantly higher than in the control animals (Fig. 2). A linear ICAM-1 staining pattern was detectable along the capillary walls and the mesangial area.

Table 1 Changes in metabolic data after induction of diabetes in rats

		0W	1W	4W	12W	24W
Body weight (g)	Control	122 ± 1.2	189 ± 7.3	366 ± 8.7	568 ± 14.6	631.7 ± 20.3
	Diabetic		162 ± 3.4*	236.4 ± 12.9*†	259 ± 33.2*	233.3 ± 18.5*
	Diabetic + insulin			329 ± 21.4		
Kidney weight (mg/g BW)	Control	5.7 ± 0.2	5.08 ± 0.2	4.1 ± 0.05	3.09 ± 0.1	2.78 ± 0.1
	Diabetic		5.95 ± 0.2	6.84 ± 0.2*†	7.14 ± 1.1*	8.08 ± 0.7*
	Diabetic + insulin			4.03 ± 0.4		
Albuminuria (mg/day)	Control	97 ± 21.1	113.7 ± 32.0	134.7 ± 11.4	136.9 ± 13.3	175.5 ± 17.1
	Diabetic		118.5 ± 11.0	815.1 ± 15.0*†	1037.8 ± 31.6	1583.1 ± 47.8*
	Diabetic + insulin			330.6 ± 44.5		
HbA1c (%)	Control	3.3 ± 0.1	3.7 ± 0.1	3.8 ± 0.6	3.6 ± 0.2	3.7 ± 0.2
	Diabetic		3.8 ± 0.2*	8.9 ± 0.5*†	10.0 ± 0.7*	9.6 ± 0.3*
	Diabetic + insulin			4.6 ± 0.3		

Data are mean ± SEM

* $p < 0.05$ vs. control

† $p < 0.05$ vs. diabetic + insulin

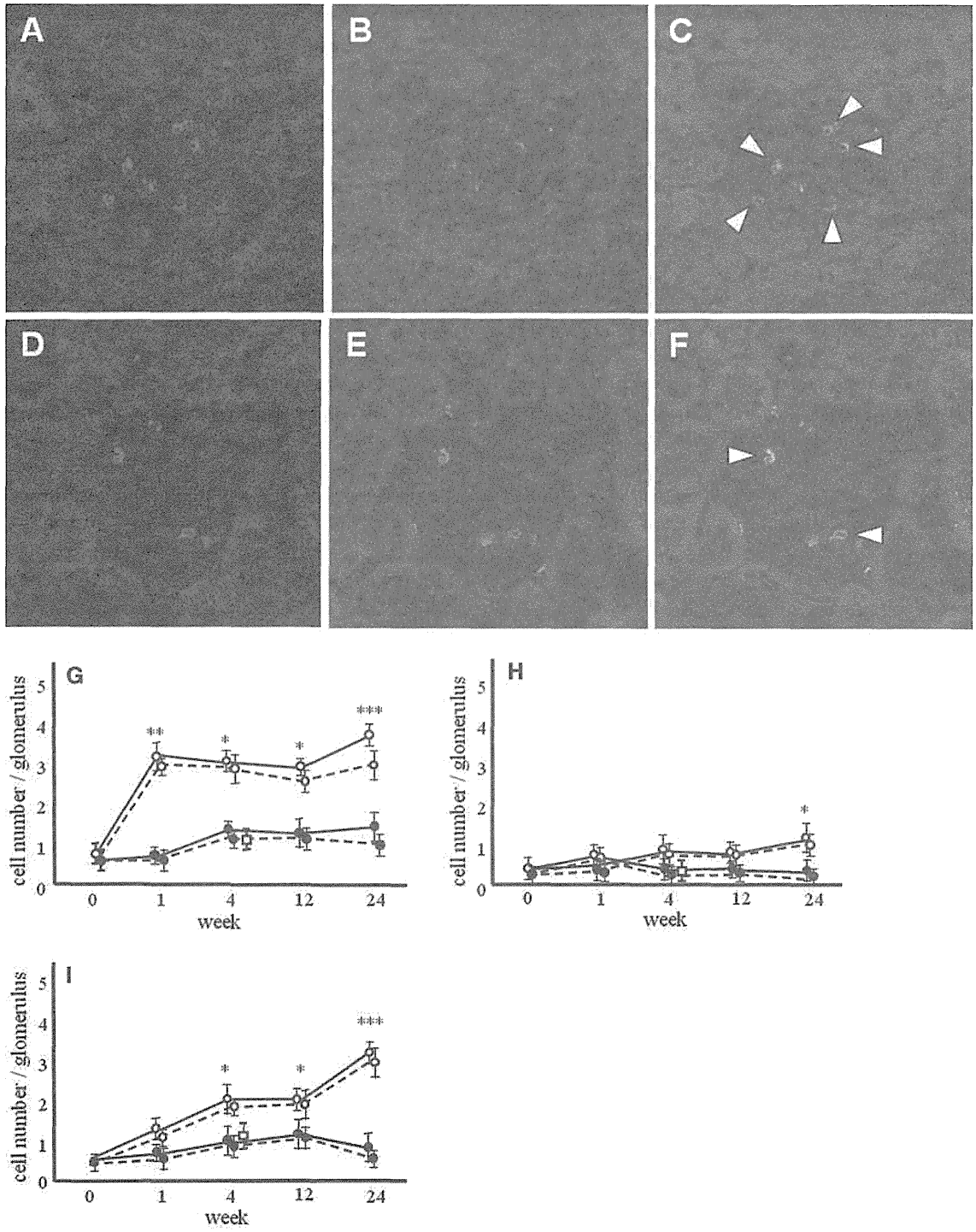

Fig. 1 Identification of macrophages in diabetic rat glomeruli. Indirect immunofluorescent micrographs from diabetic rat glomeruli 24 weeks after STZ injection, stained with anti-ED1 (pan-macrophages) (**a**), anti-ED3 (Sn-positive macrophages) (**d**), anti-OX-6 (MHC class II-positive cells) (**b**, **e**), anti-ED1 + anti-OX-6 (**c**), anti-ED3 + anti-OX-6 (**f**), magnification ×200. Intraglomerular infiltration by pan-macrophages (ED1) (**g**), resident macrophages (ED2) (**h**), and Sn-positive macrophages (ED3) (**i**) in diabetic rats (*open circle*), in control rats (*closed circle*) at 0, 1, 4, 12, and 24 weeks, and insulin-treated diabetic rats (*open square*) at 4 weeks. A *straight line* represents ED1, ED2, and ED3 and a *broken line* represents ED1, ED2, and ED3 plus OX-6. Data are means ± SEM of 50 glomeruli, respectively. $*p < 0.05$ vs. control, $**p < 0.01$ vs. control, $***p < 0.005$ vs. control

Staining for α-SMA

In control rats, α-SMA was expressed in the arterioles but not in the glomerular cells. The rate of α-SMA-positive glomeruli increased gradually, particularly from 12 to 24 weeks in diabetic rats (Fig. 3).

Staining for type IV collagen

In control rats, there was weak staining for type IV collagen throughout the experimental period. The expression of type IV collagen increased between 12 and 24 weeks in diabetic rats (Fig. 4).

Mesangial matrix area

Representative glomeruli in PAM-stained sections are shown in Fig. 5. Glomerular hypertrophy and mesangial matrix expansion were observed in diabetic rats. In STZ-induced diabetic rats, the mesangial matrix area increased significantly larger than in control rats (Fig. 5).

Effect of insulin treatment

A significantly higher body weight and lower kidney weight per body weight were observed in the insulin-treated diabetic group than in the untreated diabetic group (Table 1). After 4 weeks of insulin treatment, macrophages infiltrated into diabetic glomeruli decreased to the same level of control rats (Fig. 1), and ICAM-1 expression in the diabetic rats was comparable to that in the control rats (Fig. 2). The expression of α-SMA and type IV collagen, and mesangial matrix area were also suppressed as same as the control rats (Figs. 3, 4, 5). These results indicated that hyperglycemia but not STZ induced the infiltration of macrophages and subsequent histological changes in the glomeruli of diabetic rats.

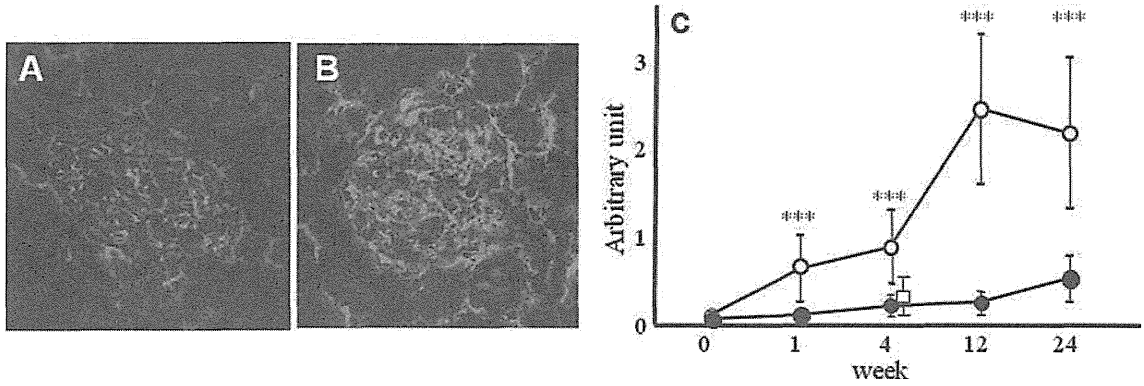

Fig. 2 Identification of ICAM-1 in diabetic glomeruli. Indirect immunofluorescent micrographs from control rats at 24 weeks (**a**) and diabetic rats at 24 weeks after STZ injection (**b**), stained with ICAM-1, magnification ×200. **c** Intraglomerular ICAM-1 expression in control rats (*closed circle*), diabetic rats (*open circle*) at 0, 1, 4, 12, and 24 weeks, and insulin-treated diabetic rats (*open square*) at 4 weeks. ***$p < 0.005$ vs. control

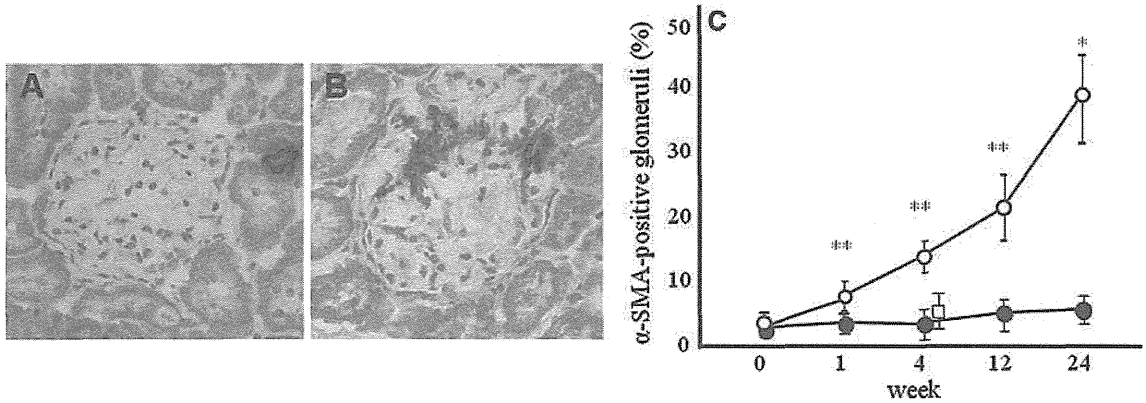

Fig. 3 Identification of α-SMA in diabetic glomeruli. Immunoperoxidase staining for α-SMA in control rats at 24 weeks (**a**) and diabetic rats at 24 weeks after STZ injection (**b**), magnification ×200. **c** Intraglomerular α-SMA expression in control rats (*closed circle*), diabetic rats (*open circle*) at 0, 1, 4, 12, and 24 weeks, and insulin-treated diabetic rats (*open square*) at 4 weeks. *$p < 0.05$ vs. control, **$p < 0.01$ vs. control

Effects of cytokines and high glucose on the expression of Sn on THP-1 cells

Sn mRNA expression was significantly increased with concentration dependency by stimulation of IL-1β and TNF-α (Fig. 6). However, Sn expression was not induced by hyperglycemic condition or stimulation with IL-4, and TGF-β1. To confirm whether IL-1β and TNF-α is upregulated in vivo, we analyzed the gene expression of IL-1β and TNF-α in the glomeruli of control and diabetic rats. As shown in Fig. 7, mRNA expression of IL-1β and TNF-α is upregulated in diabetic glomeruli. These results suggest that Sn might be induced by these inflammatory cytokines in vivo.

Discussion

Sn is expressed on a subpopulation of macrophages with a highly restricted tissue distribution in normal conditions including marginal zone macrophages of the spleen, sinus macrophages of lymph nodes, and omentum macrophages [23]. It is important to note that Sn can be rapidly induced in response to serum factors [6], glucocorticoids, and cytokines [7]. Recent studies in humans have shown that Sn can be expressed abundantly on macrophages recruited during pathological conditions including multiple sclerosis, atherosclerosis, rheumatoid arthritis, and breast cancer [8]. Therefore, Sn is suggested to relate to chronic inflammation and is considered as a marker of activated macrophages.

Only a few macrophages are seen in the glomeruli of non-diabetic control rats. On the other hand, ED1 which is expressed in pan macrophages, peaked at 1 week and maintained to 24 weeks, and most of macrophages were positive for MHC class II in the glomeruli (Fig. 1c, g). ED2 which is expressed in resident macrophages in the rats with STZ-induced diabetes [13], did not increase in diabetic glomeruli (Fig. 1h). Sn-positive macrophages continued to increase gradually and most of these macrophages are also

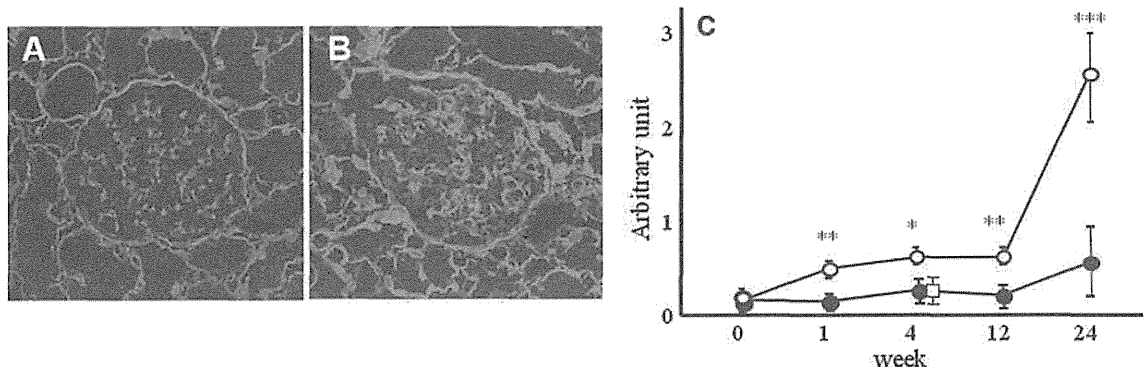

Fig. 4 Identification of type IV collagen in diabetic glomeruli. Indirect immunofluorescent micrographs from control rats at 24 weeks (**a**) and diabetic rats at 24 weeks after STZ injection (**b**), stained with type IV collagen, magnification ×200. **c** Intraglomerular type IV collagen expression in control rats (*closed circle*), diabetic rats (*open circle*) at 0, 1, 4, 12, and 24 weeks, and insulin-treated diabetic rats (*open square*) at 4 weeks. $*p < 0.05$ vs. control, $**p < 0.01$ vs. control, $***p < 0.005$ vs. control

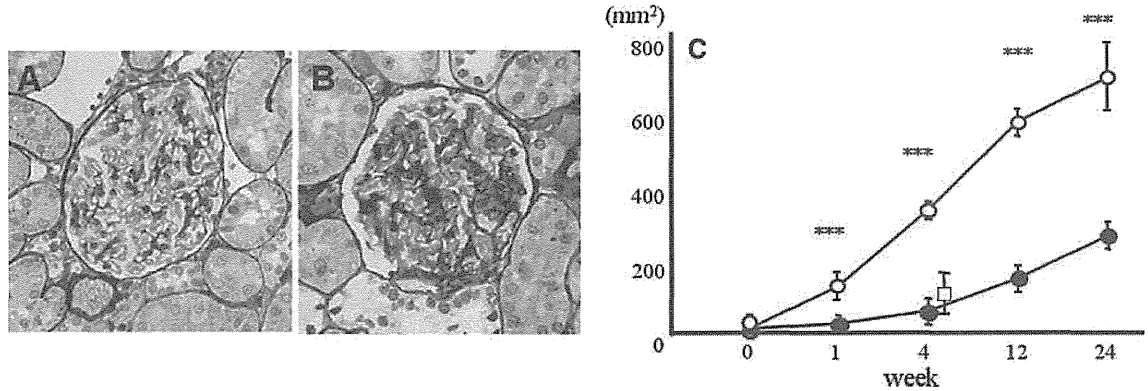

Fig. 5 Identification and quantification of PAM-positive area in diabetic glomeruli. PAM staining of kidney sections in control rats at 24 weeks (**a**) and diabetic rats at 24 weeks after STZ injection (**b**), magnification ×200. **c** Mesangial matrix area is defined as PAM-positive area in the tuft area in control rats (*closed circle*), diabetic rats (*open circle*) at 0, 1, 4, 12, and 24 weeks, and insulin-treated diabetic rats (*open square*) at 4 weeks. $***p < 0.005$ vs. control

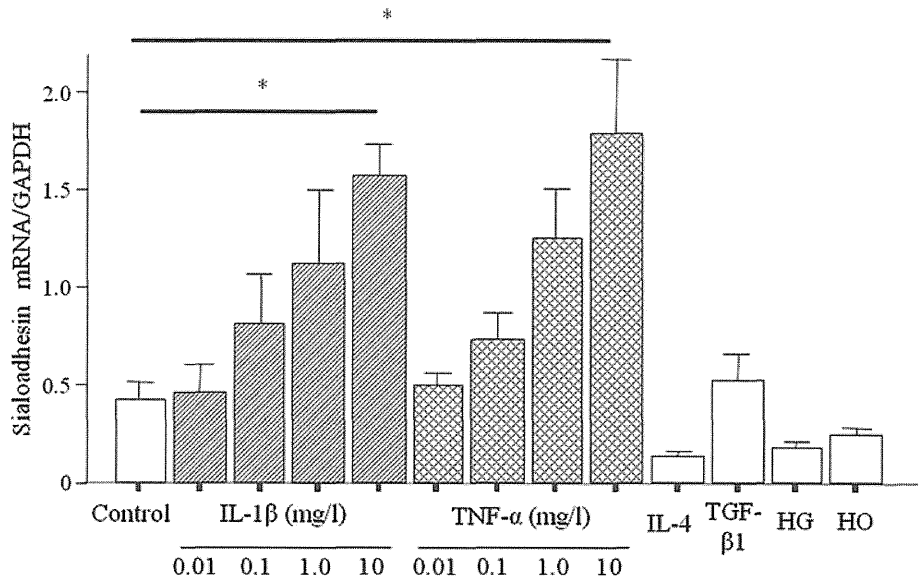

Fig. 6 Transcriptional regulation of Sn expression on THP-1 cells. Sn mRNA expression after 24 h exposure to various cytokines or hyperglycemic condition was determined by quantitative real-time RT-PCR. *HG* hyperglycemic condition, *HO* hyperosmotic control. $n = 3$ per each group. Data are mean ± SE. $*p < 0.05$ compared with vehicle (ANOVA)

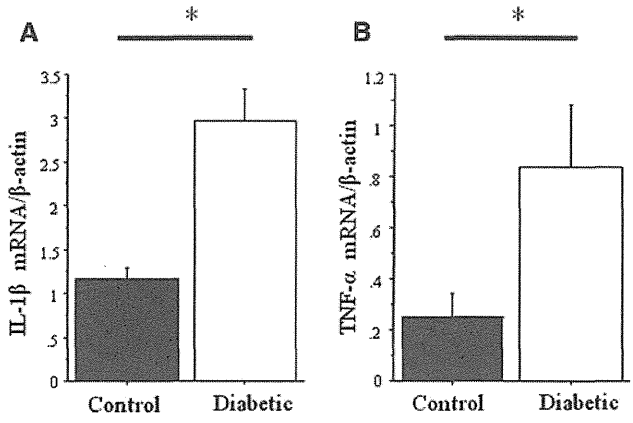

Fig. 7 Cytokine expressions in rat kidney. mRNA expression of IL-1β and TNF-α was determined by quantitative real-time RT-PCR. mRNA expression of IL-1β and TNF-α is upregulated in diabetic glomeruli. $n = 3$ per each group. Data are mean ± SE. $*p < 0.05$ compared with vehicle (ANOVA)

positive for MHC class II in the diabetic glomeruli (Fig. 1f, i). Since ICAM-1 expression was significantly upregulated in diabetic rats compared to control animals (Fig. 2), ICAM-1 may be involved in the infiltration of total and Sn-positive macrophages in diabetic glomeruli. Sn-negative activated macrophages are infiltrated in the glomeruli in the early phase of diabetic nephropathy, but the proportion of Sn-positive activated macrophages was increased during the progression of diabetic nephropathy. These results indicated that Sn-positive macrophages may contribute to chronic inflammation in diabetic nephropathy.

We further investigated the correlation of phenotypic change between macrophages and mesangial cells in the glomeruli of STZ-induced diabetic rats. α-SMA is considered as a marker for the phenotypic change of mesangial cells [20, 21] and to play a pivotal role in the accumulation of extracellular matrix in diabetic nephropathy. The rate of α-SMA-positive glomeruli increased gradually and increased particularly from 12 to 24 weeks in diabetic rats (Fig. 3). Furthermore, the expression of type IV collagen increased between 12 and 24 weeks in diabetic rats (Fig. 4), and the mesangial matrix area in diabetic rats increased significantly larger than in control rats (Fig. 5). Therefore, the phenotypic change of mesangial cells and accumulation of extracellular matrix was observed in parallel with an increase of Sn-positive macrophages.

Sn was originally defined as a sheep erythrocyte receptor on mouse macrophages [5, 6]. In both mice and humans, the cDNA for Sn encodes a 185-kDa type I transmembrane glycoprotein, made up of 17 immunoglobulin-like domains and a short cytoplasmic tail [24, 25]. Sn is a prototypic member of the Siglec family of sialic acid-binding immunoglobulin-like lectins and is also referred to as Siglec-1 [26]. Sn was designated CD169 at the seventh Human Leukocyte Differentiation Antigen workshop. The large extracellular region of Sn contains a sialic acid-binding site within the membrane-distal V-set domain and is assumed to extend away from the glycocalyx on the cell surface to mediate cell to cell interactions [27]. To investigate the mechanism of the induction of Sn in macrophages, gene expression of Sn was induced by several conditions in the THP-1 human monocytic cell line. Sn mRNA expression was significantly increased by stimulation of IL-1β and TNF-α dose dependently (Fig. 6). However, Sn expression was not induced by hyperglycemic conditions or stimulation with IL-4, and TGF-β1 (Fig. 6). Furthermore, we confirmed that mRNA expression of IL-1β and TNF-α is upregulated in diabetic glomeruli (Fig. 7). These data indicate that inflammatory

cytokines, i.e., IL-1β and TNF-α, but not hyperglycemia, stimulate the expression of Sn in macrophages.

Hyperglycemia causes glomerular hyperfiltration and glomerular hypertrophy [28, 29]. Increased intraglomerular pressure caused by hyperfiltration may activate the mesangial cells because phenotypic change of mesangial cells is brought about by mechanical stress in vitro [30]. Growth factors including insulin-like growth factor-1 (IGF-1) and platelet-derived growth factor (PDGF) are known to be involved in glomerular hypertrophy [31–33] and may play an important role in the phenotypic change of mesangial cells. Growth factors such as IGF-1 and PDGF are synthesized by macrophages, mesangial cells and others [34, 35]. From these findings, phenotypic change of mesangial cells might be caused by macrophages derived growth factors. Although our current study showed that the phenotypic change of mesangial cells was in parallel with increase of Sn-positive macrophages, the mechanism of interaction between macrophages and mesangial cells remains unclear and further studies are needed.

In conclusion, the current results suggest that macrophages are activated in diabetic glomeruli and Sn-positive activated macrophages may contribute to the progression of diabetic nephropathy through activation of mesangial cells.

Acknowledgments This study was supported in part by Grant-in-Aid for Scientific Research (C) to K. Shikata (21591031), Grant-in-Aid for Young Scientists (B) to D. Ogawa (23790942) from the Ministry of Education, Culture, Sports, Science and Technology and by Grant-in-Aid for Diabetic Nephropathy from the Ministry of Health, Labour and Welfare of Japan. This work has received support from the Takeda Science Foundation, the Naito Foundation, the Japan Foundation for Applied Enzymology, and the Ryobi Teien Memory Foundation.

References

1. Furuta T, Saito T, Ootaka T, Soma J, Obara K, Abe K, et al. The role of macrophages in diabetic glomerulosclerosis. Am J Kidney Dis. 1993;21(5):480–5.
2. Sugimoto H, Shikata K, Hirata K, Akiyama K, Matsuda M, Kushiro M, et al. Increased expression of intercellular adhesion molecule-1 (ICAM-1) in diabetic rat glomeruli: glomerular hyperfiltration is a potential mechanism of ICAM-1 upregulation. Diabetes. 1997;46(12):2075–81.
3. Okada S, Shikata K, Matsuda M, Ogawa D, Usui H, Kido Y, et al. Intercellular adhesion molecule-1-deficient mice are resistant against renal injury after induction of diabetes. Diabetes. 2003; 52(10):2586–93.
4. Crocker PR, Gordon S. Properties and distribution of a lectin-like hemagglutinin differentially expressed by murine stromal tissue macrophages. J Exp Med. 1986;164(6):1862–75.
5. Crocker PR, Gordon S. Mouse macrophage hemagglutinin (sheep erythrocyte receptor) with specificity for sialylated glycoconjugates characterized by a monoclonal antibody. J Exp Med. 1989;169(4):1333–46.
6. Crocker PR, Hill M, Gordon S. Regulation of a murine macrophage haemagglutinin (sheep erythrocyte receptor) by a species-restricted serum factor. Immunology. 1988;65(4):515–22.
7. van den Berg TK, van Die I, de Lavalette CR, Dopp EA, Smit LD, van der Meide PH, et al. Regulation of sialoadhesin expression on rat macrophages. Induction by glucocorticoids and enhancement by IFN-beta, IFN-gamma, IL-4, and lipopolysaccharide. J Immunol. 1996;157(7):3130–8.
8. Steiniger B, Barth P, Herbst B, Hartnell A, Crocker PR. The species-specific structure of microanatomical compartments in the human spleen: strongly sialoadhesin-positive macrophages occur in the perifollicular zone, but not in the marginal zone. Immunology. 1997;92(2):307–16.
9. Ito Y, Kawachi H, Morioka Y, Nakatsue T, Koike H, Ikezumi Y, et al. Fractalkine expression and the recruitment of CX3CR1+ cells in the prolonged mesangial proliferative glomerulonephritis. Kidney Int. 2002;61(6):2044–57.
10. Lan HY, Nikolic-Paterson DJ, Mu W, Atkins RC. Local macrophage proliferation in the progression of glomerular and tubulointerstitial injury in rat anti-GBM glomerulonephritis. Kidney Int. 1995;48(3):753–60.
11. Lai PC, Cook HT, Smith J, Keith JC Jr, Pusey CD, Tam FW. Interleukin-11 attenuates nephrotoxic nephritis in Wistar Kyoto rats. J Am Soc Nephrol. 2001;12(11):2310–20.
12. Ikezumi Y, Kanno K, Karasawa T, Han GD, Ito Y, Koike H, et al. The role of lymphocytes in the experimental progressive glomerulonephritis. Kidney Int. 2004;66(3):1036–48.
13. Dijkstra CD, Dopp EA, Joling P, Kraal G. The heterogeneity of mononuclear phagocytes in lymphoid organs: distinct macrophage subpopulations in the rat recognized by monoclonal antibodies ED1, ED2 and ED3. Immunology. 1985;54(3): 589–99.
14. Mauer SM, Steffes MW, Ellis EN, Sutherland DE, Brown DM, Goetz FC. Structural-functional relationships in diabetic nephropathy. J Clin Invest. 1984;74(4):1143–55.
15. Osterby R, Parving HH, Hommel E, Jorgensen HE, Lokkegaard H. Glomerular structure and function in diabetic nephropathy. Early to advanced stages. Diabetes. 1990;39(9):1057–63.
16. Makino H, Yamasaki Y, Hironaka K, Ota Z. Glomerular extracellular matrices in rat diabetic glomerulopathy by scanning electron microscopy. Virchows Arch B Cell Pathol Incl Mol Pathol. 1992;62(1):19–24.
17. Makino H, Yamasaki Y, Haramoto T, Shikata K, Hironaka K, Ota Z, et al. Ultrastructural changes of extracellular matrices in diabetic nephropathy revealed by high resolution scanning and immunoelectron microscopy. Lab Invest. 1993;68(1):45–55.
18. Abrass CK, Peterson CV, Raugi GJ. Phenotypic expression of collagen types in mesangial matrix of diabetic and nondiabetic rats. Diabetes. 1988;37(12):1695–702.
19. Makino H, Shikata K, Wieslander J, Wada J, Kashihara N, Yoshioka K, et al. Localization of fibril/microfibril and basement membrane collagens in diabetic glomerulosclerosis in type 2 diabetes. Diabet Med. 1994;11(3):304–11.
20. Johnson RJ, Iida H, Alpers CE, Majesky MW, Schwartz SM, Pritzi P, et al. Expression of smooth muscle cell phenotype by rat mesangial cells in immune complex nephritis. Alpha-smooth muscle actin is a marker of mesangial cell proliferation. J Clin Invest. 1991;87(3):847–58.
21. Alpers CE, Hudkins KL, Gown AM, Johnson RJ. Enhanced expression of "muscle-specific" actin in glomerulonephritis. Kidney Int. 1992;41(5):1134–42.
22. Kodera R, Shikata K, Kataoka HU, Takatsuka T, Miyamoto S, Sasaki M, et al. Glucagon-like peptide-1 receptor agonist ameliorates renal injury through its anti-inflammatory action without lowering blood glucose level in a rat model of type 1 diabetes. Diabetologia. 2011;54(4):965–78.

23. Takeya M, Hsiao L, Takahashi K. A new monoclonal antibody, TRPM-3, binds specifically to certain rat macrophage populations: immunohistochemical and immunoelectron microscopic analysis. J Leukoc Biol. 1987;41(3):187–95.
24. Crocker PR, Mucklow S, Bouckson V, McWilliam A, Willis AC, Gordon S, et al. Sialoadhesin, a macrophage sialic acid binding receptor for haemopoietic cells with 17 immunoglobulin-like domains. EMBO J. 1994;13(19):4490–503.
25. Hartnell A, Steel J, Turley H, Jones M, Jackson DG, Crocker PR. Characterization of human sialoadhesin, a sialic acid binding receptor expressed by resident and inflammatory macrophage populations. Blood. 2001;97(1):288–96.
26. Crocker PR, Varki A. Siglecs, sialic acids and innate immunity. Trends Immunol. 2001;22(6):337–42.
27. Crocker PR, Hartnell A, Munday J, Nath D. The potential role of sialoadhesin as a macrophage recognition molecule in health and disease. Glycoconj J. 1997;14(5):601–9.
28. Wiseman MJ, Viberti GC, Keen H. Threshold effect of plasma glucose in the glomerular hyperfiltration of diabetes. Nephron. 1984;38(4):257–60.
29. Osterby R, Gundersen HJ. Fast accumulation of basement membrane material and the rate of morphological changes in acute experimental diabetic glomerular hypertrophy. Diabetologia. 1980;18(6):493–500.
30. Harris RC, Haralson MA, Badr KF. Continuous stretch-relaxation in culture alters rat mesangial cell morphology, growth characteristics, and metabolic activity. Lab Invest. 1992;66(5):548–54.
31. Miyatake N, Shikata K, Wada J, Sugimoto H, Takahashi S, Makino H. Differential distribution of insulin-like growth factor-1 and insulin-like growth factor binding proteins in experimental diabetic rat kidney. Nephron. 1999;81(3):317–23.
32. Floege J, Topley N, Hoppe J, Barrett TB, Resch K. Mitogenic effect of platelet-derived growth factor in human glomerular mesangial cells: modulation and/or suppression by inflammatory cytokines. Clin Exp Immunol. 1991;86(2):334–41.
33. Fukui M, Nakamura T, Ebihara I, Makita Y, Osada S, Tomino Y, et al. Effects of enalapril on endothelin-1 and growth factor gene expression in diabetic rat glomeruli. J Lab Clin Med. 1994; 123(5):763–8.
34. Shimokado K, Raines EW, Madtes DK, Barrett TB, Benditt EP, Ross R. A significant part of macrophage-derived growth factor consists of at least two forms of PDGF. Cell. 1985;43(1):277–86.
35. Ross R, Raines EW, Bowen-Pope DF. The biology of platelet-derived growth factor. Cell. 1986;46(2):155–69.